

SLOVAK UNIVERSITY OF TECHNOLOGY  
BRATISLAVA

FACULTY OF ELECTRICAL ENGINEERING AND  
INFORMATION TECHNOLOGY

ELECTRIC MEASUREMENTS ON CRYSTALLINE  
SILICON CONCENTRATION CELLS

DIPLOMA THESIS

Bratislava  
February 2008

David Garrido Diez

## Declaration

The work resulting into this diploma thesis has been performed at Department of Electrotechnology SUT, FEI in Bratislava, Slovakia. Hereby I confirm that I was working on diploma thesis alone under the supervision of doc. Ing. Vladimír Šaly, PhD. and all the literature sources I have used are cited in References.

.....

Signature.

Index:

<b>1. Summary .....</b>	<b>4</b>
<b>2. Theory .....</b>	<b>5</b>
2.1. <i>Introduction</i> .....	5
2.2. <i>The solar cell</i> .....	5
2.2.1. Structure and materials of the solar cell.....	5
2.2.1.1. Structure .....	5
2.2.1.2. Devices and Materials .....	6
2.2.2. Operating principles .....	8
2.3. <i>Photogeneration of current</i> .....	9
2.3.1. Absorption of light and generation of carriers .....	10
2.3.2. Collection of current .....	13
2.3.3. Quantum efficiency .....	14
2.4. <i>Dark current</i> .....	15
2.5. <i>Characteristic I-V curve under illumination</i> .....	17
2.5.1. Short-circuit current and open-circuit voltage .....	18
2.5.2. Maximum-power point .....	19
2.5.3. Fill factor and energy conversion efficiency.....	20
2.6. <i>Equivalent circuit of a solar cell</i> .....	21
2.6.1. Equivalent circuit of the ideal device .....	21
2.6.2. Series and parallel resistances .....	22
2.7. <i>Variations from the basic behaviour</i> .....	24
2.7.1. The effect of temperature.....	24
2.7.2. The effect of illumination intensity .....	25
<b>3. Experimental.....</b>	<b>28</b>
3.1. <i>Dark I-V measurements of solar cells</i> .....	28
3.1.1. Introduction .....	28
3.1.2. Experimental details. ....	32
3.1.2.1. Samples .....	32
3.1.2.2. Connections for DC measurements. ....	34
3.1.3. Results.....	35
3.2. <i>Measurement of solar cells AC parameters</i> .....	42
3.2.1. Introduction .....	42
3.2.2. Experimental details. ....	44
3.2.2.1. Samples. ....	44
3.2.2.2. Connections for AC measurements. ....	44
3.2.3. Results.....	45
<b>4. Conclusions: .....</b>	<b>51</b>
<b>5. References: .....</b>	<b>52</b>
<b>6. Annex: .....</b>	<b>53</b>

# 1. Summary

The aim of this project has been to measure and analyse of solar cells electrical parameters. To achieve that, two ways of measuring have been realized: dark  $I-V$  measurements and AC measurements.

The current-voltage  $I-V$  characteristics of solar cells at different temperatures were measured in the dark. A one and two diodes equivalent model was used to describe the electronic properties of the solar cells. The diode ideality factors, the series and shunt resistance, that determine the fill factor and the efficiency of the solar cell, have been estimated.

The AC measurements, based on the behaviour of the solar cell applied on dark condition by AC signal, have also found useful for the determination of some parameters, like the series resistance  $R_S$ , the shunt resistance  $R_{SH}$  and the capacitance  $C$ , that have often used to model the behaviour of the solar cell.

Firstly this work starts with some theory of solar cells to take contact with this technology before the experiments and results being presented.

## **2. Theory**

### **2.1. Introduction**

The conversion of the energy carried by optical electromagnetic radiation into electrical energy is a physical phenomenon known as the photovoltaic effect. Solar cells are without doubt the most important type of device for carrying out such conversion. The use of solar cells for photovoltaic energy production on earth is now becoming the subject of growing attention. Not only at the research and development level is this happening. Many practical applications are also emerging. The aim of such projects is to build photovoltaic systems at an acceptable cost, so that electricity can be produced competitively and renewably.

### **2.2. The solar cell**

When sunlight falls on certain materials known as semiconductors, the photons making up the sunlight can transmit their energy to the valence electrons.

Each time a photon breaks a bond, an electron becomes free to roam through the lattice. The absent electron leaves behind a vacancy, or hole, that can also move through the lattice as electrons shuffle around it. In many respects these holes behave as particles in their own right, similar to the electrons but with positive charge. The movement of the electrons and holes in opposite directions generates an electric current in the semiconductor. The current can carry on through an external circuit, allowing the energy absorbed from the light to be dissipated in some useful way. To separate the electrons from the holes and prevent the bonds from reforming, an electrical field is used. It provides a force propelling the electrons and holes in opposite directions. The result is a current in the direction of this field.[1]

#### **2.2.1. Structure and materials of the solar cell**

##### **2.2.1.1. Structure**

In conventional solar cells, the electrical field is created at the junction between two regions of a crystalline semiconductor having contrasting types of conductivity (Figure 2.1). If the semiconductor is silicon, one of these regions (the *n*-type) is doped with phosphorus, which has five valence electrons (one more than silicon). This region has a much higher concentration of electrons than of holes. The other region (the *p*-type) is doped with boron, having three valence electrons (one less than silicon). Here the concentration of holes is greater. The large difference in concentrations from one region to another causes a permanent electric field directed from the *n*-type region towards the *p*-type region. This is the field responsible for separating the additional electrons and holes produced when light shines on the cell.

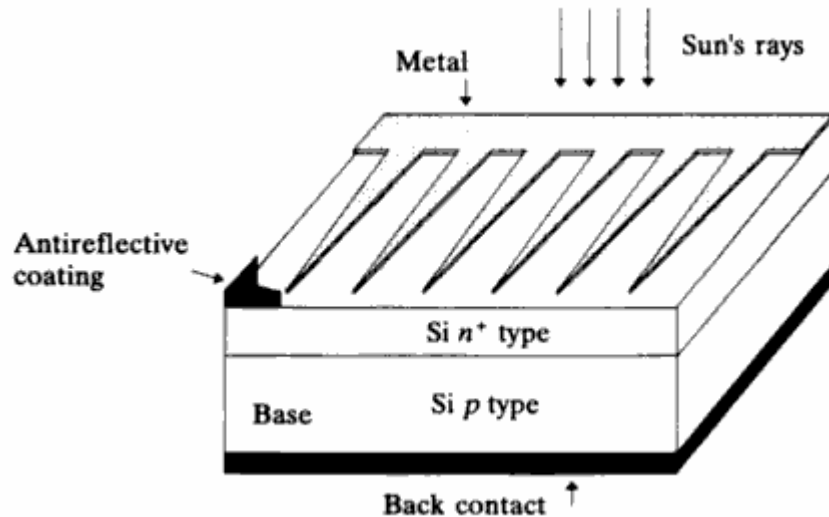


Figure 2.1 Structure of a conventional solar cell

Nearly all cells currently available have a  $p-n$  junction of this type. In silicon cells (the most common type of solar cell) the junction is obtained by diffusing phosphorus into a wafer of silicon previously doped with boron. The junction is very shallow, typically only about 0.2 to 0.5  $\mu\text{m}$  deep. This shallow, diffused layer is commonly called the emitter. The electrical contact with the illuminated side of the cell (the side where the diffusion is done) has to leave most of the surface uncovered otherwise light cannot enter the cell. However, the electrical resistance of the contact must not be too high. The compromise usually adopted is to use contacts with the form of a comb, as seen in Figure 2.1. In contrast, the electrical contact on the dark side of the cell covers the whole surface of the cell. Usually, an antireflective coating is applied to the illuminated side to increase the fraction of incident light absorbed.[2]

## 2.2.1.2. Devices and Materials

### 2.2.1.2.1. Homojunction Devices

Crystalline silicon for example. A single material—crystalline silicon—is altered so that one side is  $p$ -type, and the other side is  $n$ -type. The  $p-n$  junction is located so that the maximum amount of light is absorbed near it. The free electrons and holes generated by light deep in the silicon go to the  $p-n$  junction then separate to produce a current if the silicon is of sufficient high quality.

In this homojunction design there are many aspects to increase conversion efficiency:

- ✓ Depth of the  $p/n$  junction below the cell's surface
- ✓ Amount and distribution of dopant atoms on either side of the  $p/n$  junction
- ✓ Crystallinity and purity of the silicon.

### 2.2.1.2.2. Heterojunction Devices

The junction is formed by contacting two different semiconductors—  $\text{CIS}$ ,  $\text{CdS}$  and  $\text{CuInSe}_2$ . This structure is often chosen for producing cells made of thin-film

materials that absorb light much better than silicon. The top and bottom layers in a heterojunction device have different roles. The top layer is a material with a high bandgap selected for its transparency to light that allows almost all incident light to reach the bottom layer, which is a material with low bandgap that readily absorbs light. This light then generates electrons and holes very near the junction, which helps to effectively separate the electrons and holes before they can recombine.

Advantages:

- ✓ Over homojunction devices, which require materials that can be doped both p- and n-type. Many PV materials can be doped either *p*-type or *n*-type, but not both.
- ✓ High-bandgap window layer reduces the cell's series resistance. The window material can be made highly conductive, and the thickness can be increased without reducing the transmittance of light. As a result, light-generated electrons can easily flow laterally in the window layer to reach an electrical contact.

2.2.1.2.3. *p-i-n* and *n-i-p* Devices

- ✓ *p-i-n*: Amorphous silicon thin-film cells.
- ✓ *n-i-p* : *CdTe* cells.

Three-layer is created, with a middle intrinsic (*i*-type or undoped) layer between an *n*-type layer and a *p*-type layer.

Light generates free electrons and holes in the intrinsic region, which are then separated by the electric field.

In the *p-i-n* amorphous silicon (*a-Si*) cell, the top layer is *p*-type *a-Si*, the middle layer is intrinsic silicon, and the bottom layer is *n*-type *a-Si*. In a *CdTe* cell, the device structure is similar to the *a-Si* cell, except the order of layers is flipped upside down. Specifically, in a typical *CdTe* cell, the top layer is *p*-type cadmium sulphide (*CdS*), the middle layer is intrinsic *CdTe*, and the bottom layer is *n*-type zinc telluride (*ZnTe*).

Disadvantages:

- ✓ Amorphous silicon has many atomic-level electrical defects(traps) when it is high current zone. This makes that a very little current would flow if an *a-Si* cell had to depend on diffusion current.

Advantages:

- ✓ In a *p-i-n(n-i-p)* cell, current flows because the free electrons and holes are generated within the influence of an electric field, rather than having to move toward the field.

2.2.1.2.4. Multijunction Devices

Individual cells with different bandgaps are stacked on top of one another. The individual cells are stacked in such a way that sunlight falls first on the material having the largest bandgap(*GaAs*).

This structure can achieve a higher total conversion efficiency by capturing a larger portion of the solar spectrum. In the typical multijunction cell photons not

absorbed in the first cell are transmitted to the second cell, which then absorbs the higher-energy portion of the remaining solar radiation while remaining transparent to the lower-energy photons.

Disadvantages:

- ✓ A multijunction cell can be made in two different ways. And both are too expensive in terms of energy.
- ✓ In the mechanical stack approach, two individual solar cells are made independently, one with a high bandgap and one with a lower bandgap. Then the two cells are mechanically stacked, one on top of the other.
- ✓ In the monolithic approach, one complete solar cell is made first, and then the layers for the second cell are grown or deposited directly on the first. This multijunction device has a top cell of gallium indium phosphide, then a "tunnel junction" to allow the flow of electrons between the cells, and a bottom cell of gallium arsenide.

Advantages:

- ✓ These cells have efficiencies of more than 35% under concentrated sunlight.

### 2.2.2. Operating principles

If a solar cell is connected to a load and illuminated, as shown in Figure 2.2, a difference in potential will be produced across the load and current will circulate. The current leaves the cell from the positive terminal and returns to the negative terminal. Under such operating conditions the cell functions as a generator of energy. This is what makes it so interesting. The processes going on inside the cell can be described as follows:

- ✓ Photons that reach the interior of the cell and have an energy equal to or greater than the bandgap are absorbed in the bulk of the semiconductor, generating electron-hole pairs that can function as carriers of current.
- ✓ The electric field, or potential difference, produced by the  $p-n$  junction is responsible for separating the carriers before they have a chance to recombine. The result is a potential difference and current in the external circuit including the load.
- ✓ The presence of a potential difference across the terminals of the device produces, as in any device based on  $p-n$  junctions, the phenomena of injection and recombination of electron-hole pairs. In the solar cell these amount to losses. The extent of the losses depends on this potential difference.



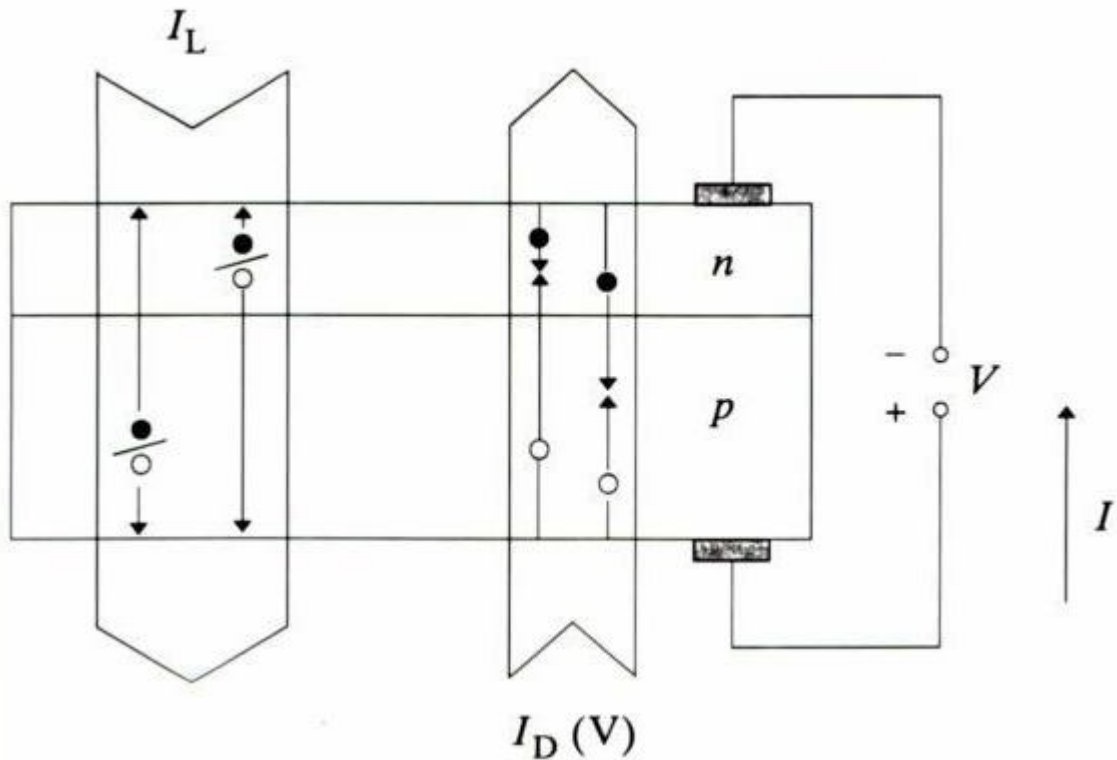


Figure 2.2. Internal currents in a solar cell. The unshaded circles represent holes and the black circles represent electrons.[2]

In summary, when a load is connected to an illuminated solar cell the current that flows is the net result of two counteracting components of internal current:

- ✓ The photogenerated current or simply photocurrent,  $I_L$ , due to the generation of carriers by the light.
- ✓ The diode or dark current,  $I_D$ , due to the recombination of carriers driven by the external voltage. This voltage is needed to deliver power to the load.

Let us assume that the two currents can be superimposed linearly, as turns out to be true in many practical instances. Then the current in the external circuit can be calculated as the difference between the two components. Taking the photocurrent as positive, we can write:

$$I = I_L - I_D(V) \quad (2.1)$$

This is the fundamental characteristic equation of a solar cell. It is valid over all operating conditions, even when the device functions as a diode, dissipating rather than generating electricity, in which case the recombination outweighs the photogeneration.

### 2.3. Photogeneration of current

Solar radiation contains photons of all energies according to the spectral distribution shown in Figure 2.3. Just beyond the earth's atmosphere, the solar spectrum

(called AM0, zero relative air mass) is similar to that of a black body at 5800 K and has an irradiance of 136.7 mW/cm<sup>2</sup>. At sea level, under clear conditions, atmospheric absorption modifies the spectrum typically to AM1.5 (1.5 relative air mass) and the irradiance is reduced to 100 mW/cm<sup>2</sup> under clear conditions.

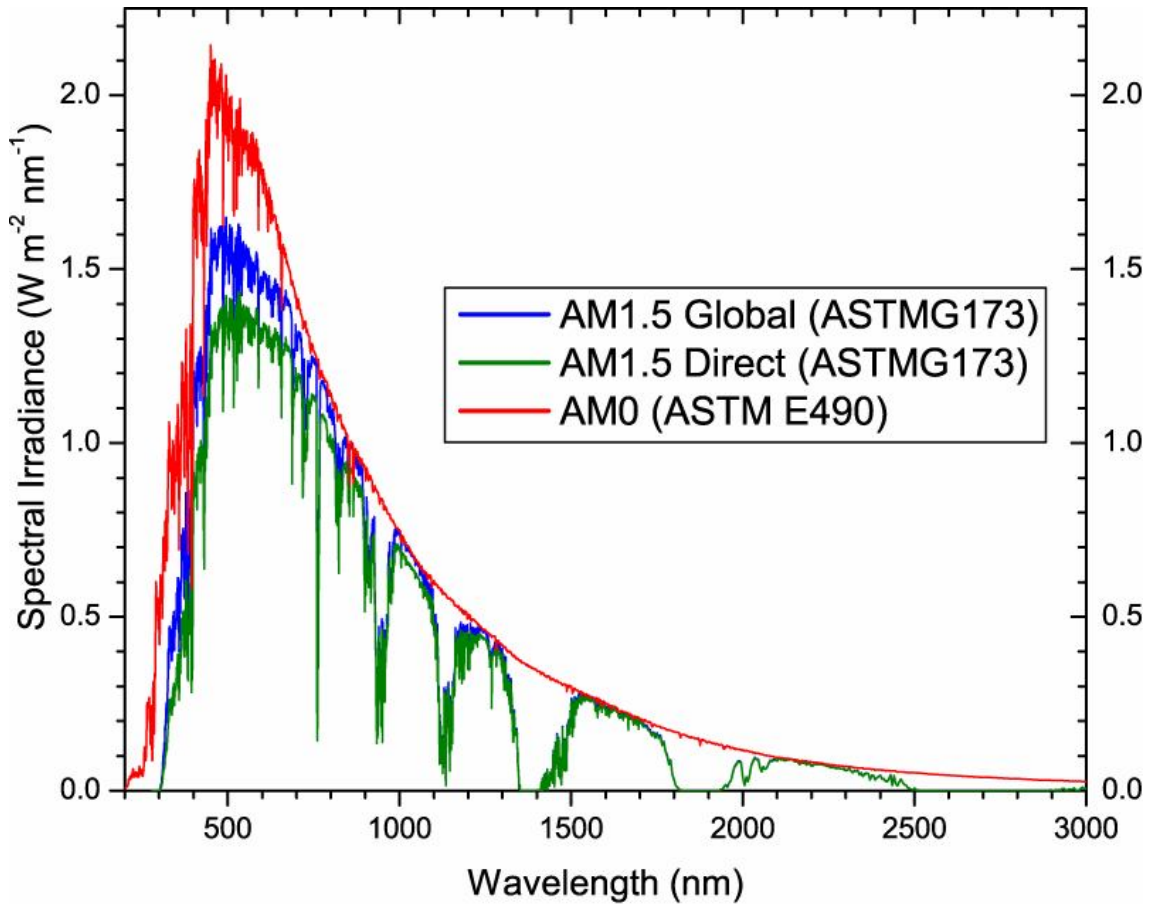


Figure 2.3: Spectral composition of solar radiation

### 2.3.1. Absorption of light and generation of carriers

A solar cell essentially consists of a semiconductor material, having a certain bandgap  $E_G$  and thickness  $W$ , as shown in Figure 2.4. Electrons of the valence band can absorb the energy of the photons falling on this semiconductor. They are promoted to the conduction band. Carriers are therefore generated by the photon absorption. Unfortunately, not all the incident photons undergo absorption and contribute to photogeneration. The reasons for this are as follows:[2]

- ✓ Photons with energy below  $E_G$  cross the semiconductor without being absorbed (the absorption coefficient is zero). This is apparent from the graphs of the optical absorption coefficient shown in Figure 2.5 for some semiconductors of interest. The resulting losses are called nonabsorption losses.
- ✓ Due to the finite value of the absorption coefficient  $\alpha(E)$  and the finite thickness  $W$  of the semiconductor, even with the photons of energy greater than  $E_G$ , a certain fraction cross the device without being absorbed. That is to say, the transmittance  $\tau(E, W)$  is always greater than zero, producing certain transmission losses.

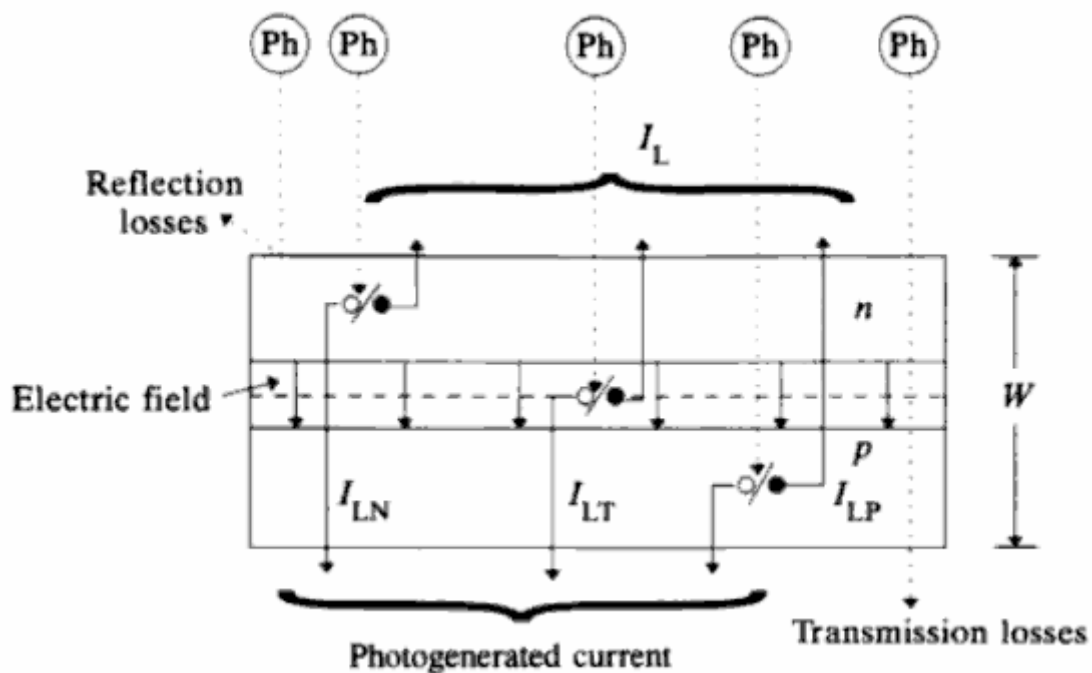


Figure 2.4. Illustration of the photogeneration of current in a solar cell. The circles marked Ph represent photons.[2]

- ✓ A certain fraction of photons of all energies are reflected on hitting the surface of the semiconductor, due to the difference in refractive index. Thus there is a reflectance  $\rho(E, W)$  greater than zero, producing reflection losses.

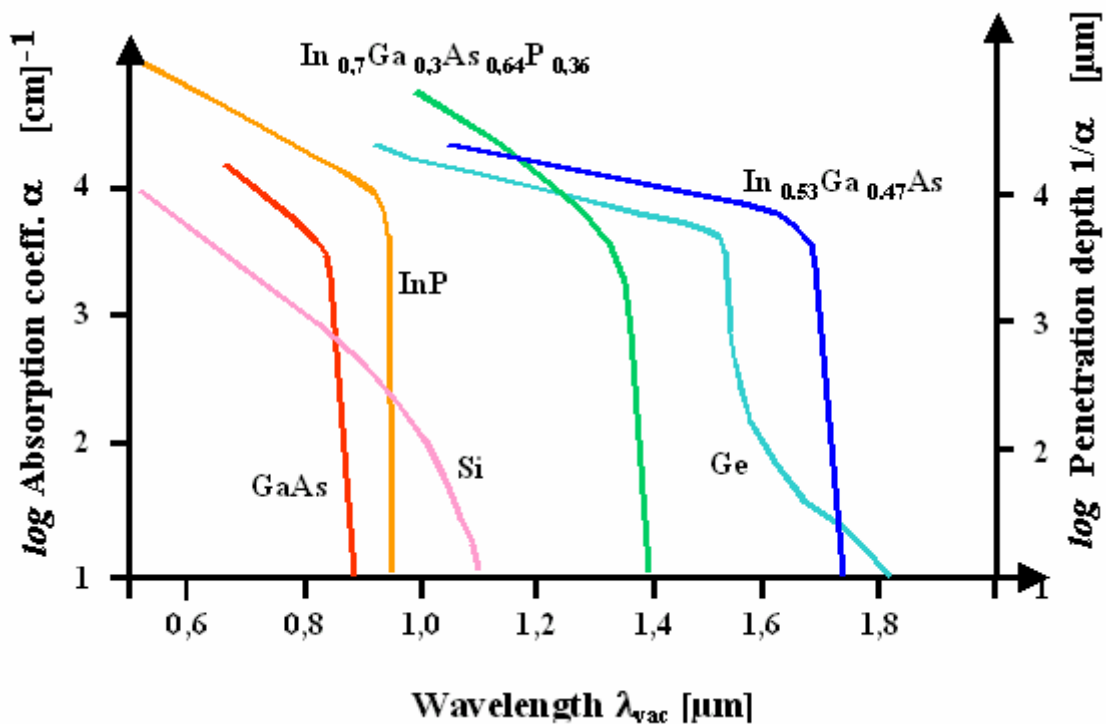


Figure 2.5. Optical absorption coefficient of some semiconductors

Only one electron-hole pair is created for each photon absorbed, whatever the energy of the photon. Thus the number of photogenerated pairs is equal to the number of photons absorbed. If we use  $\alpha'(E, W)$  to denote the spectral absorbance, the photogenerated current may be calculated from the following integral:

$$\begin{aligned} I_L &= eA_C \int_{E_G}^{\infty} S(E)\alpha'(E, W)dE \equiv \\ &\equiv eA_C \int_{E_G}^{\infty} S(E)[1 - \rho(E, W) - \tau(E, W)]dE \end{aligned} \quad (2.2)$$

where  $S(E)$  is the number of photons of energy  $E$  incident on the cell per unit area, and  $A_C$  is the area of the illuminated cell.

The nonabsorption losses are inevitable and depend only on the properties of the semiconductor. On the other hand, the reflection and transmission losses may at least in principle be reduced to zero, for example by using antireflective coatings and by suitable device design. It follows that the maximum photocurrent that can be expected from a solar cell may be obtained by discounting reflection and transmission losses. It then reaches the theoretical maximum of:

$$I_L \leq eA_C \int_{E_G}^{\infty} S(E)dE \quad (2.3)$$

The above current depends only on the bandgap and the solar spectrum, as shown in Figure 2.6. As can be seen, the current decreases as  $E_G$  is increased, and for two of the most important semiconductors, silicon and gallium arsenide, values corresponding to various illuminating spectra are indicated in this figure.

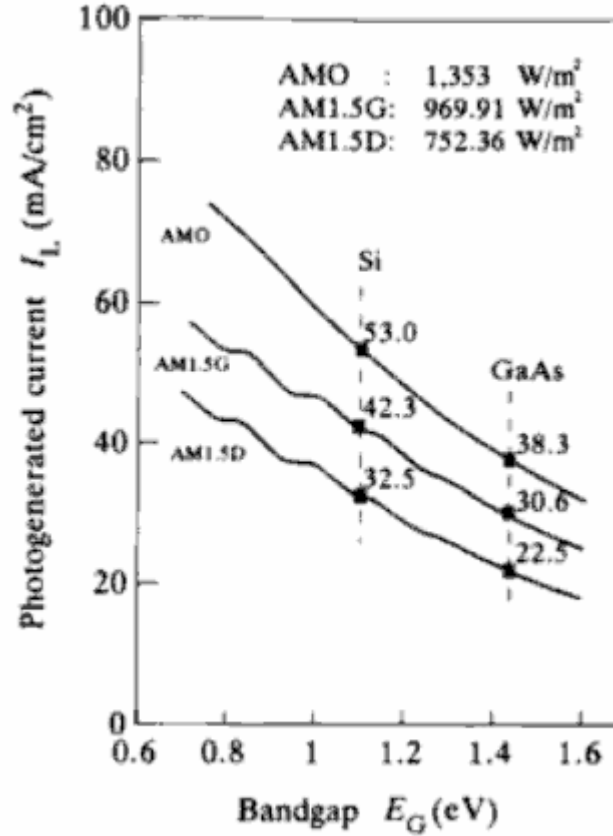


Figure 2.6 Maximum current that can be generated in a solar cell, as a function of a band gap of the semiconductor and the spectrum.[2]

### 2.3.2. Collection of current

However, not all the photogenerated carriers contribute to the external current and are useful in generating electricity. This is because, even if no external voltage exists across the device (short-circuit conditions), a small fraction of the photogenerated carriers are generated far from the area of high electric field. They then have to travel some distance towards it before being separated and collected across the junction. The fraction of the carriers that is collected is termed the collection efficiency,  $\eta_{col}(E)$ , and depends on the electrical and optical characteristics of the material and the structure of the device. Therefore, the photocurrent should be calculated as:

$$I_L = eA_C \int_{E_G}^{\infty} S(E)\alpha'(E)\eta_{col}(E)dE \quad (2.4)$$

The collection efficiency depends on which region of the device is considered. The electrons and holes generated in the space-charge zone (or transition zone), are separated and dragged by the high field in this zone towards the quasi-neutral zones as shown schematically in Figure 2.4. Thus, the electrons are dragged into the  $p$ -type zone and the holes into the  $n$ -type zone. It is a question of majority carriers being injected into these zones and migrating, mainly by drift, towards the contacts. The component of photogenerated current originating in the transition region is denoted  $I_{LT}$  in Figure 2.4.

In the quasi-neutral zones, the electric fields are very weak and the movement of minority carriers is governed by diffusion. Carriers generated in these zones diffuse towards the transition zone and towards the contacts and surface of the cell. In the  $n$  zone, for example, the electrons are repelled by the electric field of the transition zone which they are prevented from crossing. It forms, in other words, a potential barrier. However, they can move towards the contacts and surface. In contrast, most of the holes generated in the  $n$  zone diffuse toward the edge of the transition zone. There, they are collected and dragged by the electric field (they descend the potential barrier), to be injected into the  $p$  zone. Then they are in the majority and are redistributed and transported by drift. The field (the potential barrier) of the junction acts again as a separator of carrier types.[2]

It produces another component  $I_{LN}$  of the photocurrent, as indicated in Figure 2.4. An exactly similar description applies to the electrons and holes generated in the  $p$ -type neutral zone, and these give rise to a component  $I_{LP}$  of the photocurrent. It is important to point out that these processes of transport and current extraction are governed by certain finite parameters (mobilities, diffusion coefficients, etc.). Therefore, not all of the photogenerated carriers are separated by the electric field of the junction and not all contribute to the photocurrent. A fraction of them, which in a good design should be minimized, recombines in the bulk and surface of the device. This recombination produces heat and is useless for generating current and power in the load. In other words, the collection efficiency of the neutral zones (and hence of the whole device) is less than one.[3]

### 2.3.3. Quantum efficiency

For the experimental characterization of solar cells, it is useful to introduce a new parameter known as the quantum efficiency. It represents the number of electrons extracted from the cell (under short-circuit conditions) for each incident photon. Defined as such, the function  $\eta_{qe}(E)$  is sometimes termed more precisely the external quantum efficiency. This is, of course, a characteristic of the device. It is also useful to consider an internal quantum efficiency  $\eta_{qi}(E)$ . This refers to the photons that are not reflected but reach the interior of the device (it is assumed that these are not transmitted right through the device):

$$\eta_{qi}(E) \equiv \frac{I_L(E)}{eA_C S(E)[1 - \rho(E, W)]} \quad (2.5)$$

That is to say that the internal spectral response is not affected by the reflection properties of the cell surface and by possible antireflective coatings. As a function of the internal quantum efficiency, the photocurrent may be calculated as:

$$I_L = eA_C \int_{E_g}^{\infty} S(E) \eta_{qe}(E) \equiv eA_C \int_{E_g}^{\infty} S(E) [1 - \rho(E, W)] \eta_{qi}(E) dE \quad (2.6)$$

Comparing the above with equation (2.4) evidently  $\eta_{qe}(E) = \alpha(E) \eta_{col}(E)$ . The quantum efficiency represents, therefore, the product of photogeneration and collection of carriers.

The quantum efficiency is a quantity of great practical importance when it comes to characterizing the internal behaviour of solar cells. It is easily measured by illumination of the cell with monochromatic light of a known wavelength and measurement of the short-circuit current generated. Of course, its value is always less than 1. However, for many cells of practical interest, it can be very close to 1 over a fairly wide range of energies. In such cells the short-circuit current does not fall far below the maximum values shown by the curves in Figure 2.6.

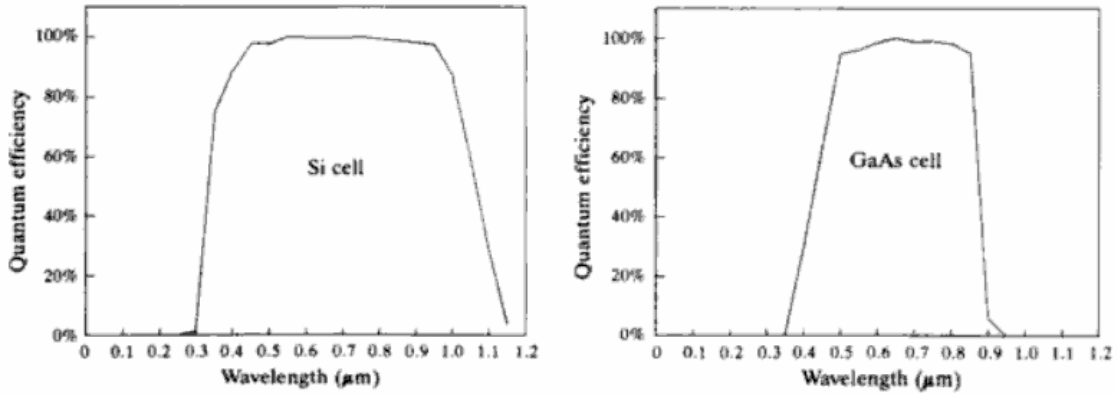


Figure 2.7. Quantum efficiency versus wavelength for solar cells made of different materials.[1]

In Figure 2.7, we present the spectral quantum efficiencies of a *Si* and a *GaAs* cell. For photons of energy below  $E_G$  (that is, wavelengths longer than  $\lambda = hc/E_G$ , where  $h$  and  $c$  are Planck's constant and the velocity of light, respectively) the cells are transparent and the response is zero. For photons of very high energy (that is, short wavelengths) absorption is produced very close to the surface. Many of the photogenerated carriers recombine before being collected as photocurrent. This explains the sudden fall in the response seen at high energies in Figure 2.7.

## 2.4. Dark current

The external voltage necessary to deliver energy to the load produces a bias across the solar cell and currents as occur in any *p-n* junction diode even when not subject to illumination, i.e. in the dark.

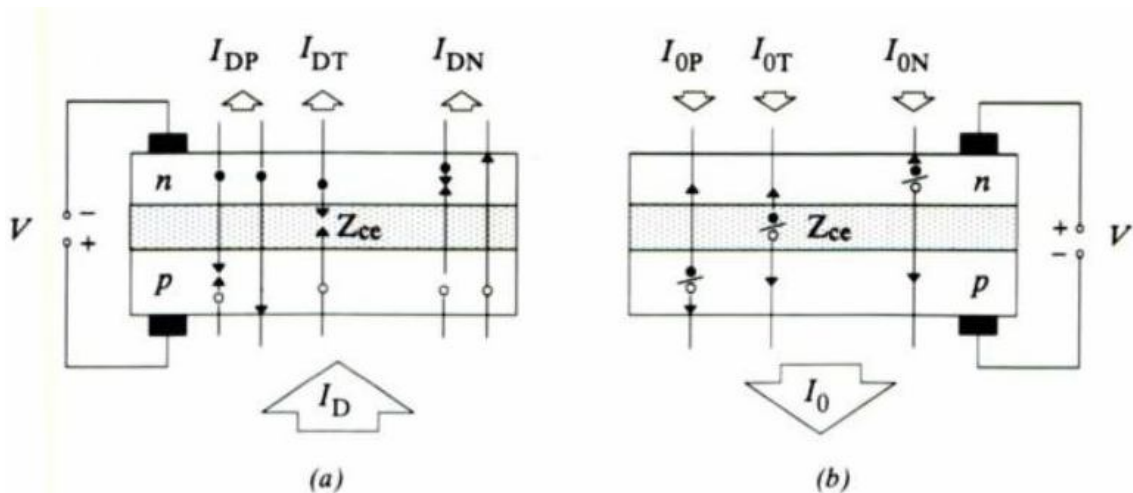


Figure 2.8. Internal components of the bias current [1]

A positive bias voltage  $V$  (measured from the  $p$  to the  $n$  zone) produces an injection of minority carriers into both sides of the transition zone. This is a consequence of the reduction of the potential barrier of the junction. Electrons from the  $n$  side are injected into the  $p$  side where they become minority carriers and move by diffusion until they recombine with holes. Recombination may occur either in the bulk of the material or in the surface of the  $p$  side. This movement of carriers is illustrated schematically in Figure 2.8 and constitutes one component of current in the diode, which we will denote as  $I_{DP}(V)$ . In an analogous way, there arise two other components of current:  $I_{DN}(V)$ , due to the recombination of the holes injected in the emitter (i.e. the  $n$  side) and  $I_{DT}(V)$ , due to the recombination of both electrons and holes in the transition zone. Figure 2.8(a) shows these components also.

If the bias voltage is negative ( $V < 0$ ) then the concentrations of carriers at both sides of the transition zone decrease, as a consequence of the increase in the potential barrier across the junction. Thermal generation of electron-hole pairs occurs, and these are extracted by the field at the junction, in a similar manner to the collection of photogenerated carriers. The reverse bias currents, which we denote as  $I_{ON}$ ,  $I_{OP}$  and  $I_{OT}$ , pass through the external circuit from the  $p$  to the  $n$  side, as shown in Figure 2.8(b). These currents add to the photocurrent when it exists, but their values are very small in comparison, and they may generally be ignored.

The currents corresponding to recombination current in the neutral zones, i.e. the diffusion currents, vary exponentially with the bias voltage. This is known as the Shockley equation for an ideal diode:

$$I_{DN}(V) + I_{DP}(V) = (I_{ON} + I_{OP}) \left[ \exp\left(\frac{eV}{kT}\right) - 1 \right] \equiv I_{01} \left[ \exp\left(\frac{eV}{kT}\right) - 1 \right] \quad (2.7)$$

where  $k$  is Boltzmann's constant and  $T$  is the absolute temperature. The component corresponding to generation and recombination in the transition zone also follows an exponential law, but a different one to the above:

$$I_{DT}(V) = I_{OT} \left[ \exp\left(\frac{eV}{2kT}\right) - 1 \right] \equiv I_{02} \left[ \exp\left(\frac{eV}{2kT}\right) - 1 \right] \quad (2.8)$$

$I_{01}$  and  $I_{02}$  are known as the reverse saturation currents. Values of  $I_{01} \sim 10^{-12}$  A  $\text{cm}^{-2}$  and  $I_{02} \sim 10^{-7} - 10^{-8}$  A  $\text{cm}^{-2}$ , are typical for monocrystalline  $\text{Si}$  cells at ambient temperatures. With these values, it is easy to check (see Figure 2.9) that the component of recombination in the transition zone is greater at low voltages ( $= < 0.4$  V). At higher voltages typical of normal operating conditions, the diffusion term becomes more important. Therefore, a good approximation is to use only the diffusion current. Otherwise, a single exponential formula of the type:

$$I_D(V) = I_0 \left[ \exp\left(\frac{eV}{mkT}\right) - 1 \right] \quad \text{with} \quad 1 < m < 2 \quad (2.9)$$



may be used to represent the sum of equations (2.7) and (2.8). At low voltages  $m \rightarrow 2$  and  $I_0 \rightarrow I_{02}$ , whereas at high voltages  $m \rightarrow 1$  and  $I_0 \rightarrow I_{01}$ . In the transition between behaviour dominated by recombination in the space charge zone and behaviour dominated by diffusion in the neutral zones,  $I_0$  and  $m$  depend on  $V$  and do not have physical meanings of their own.

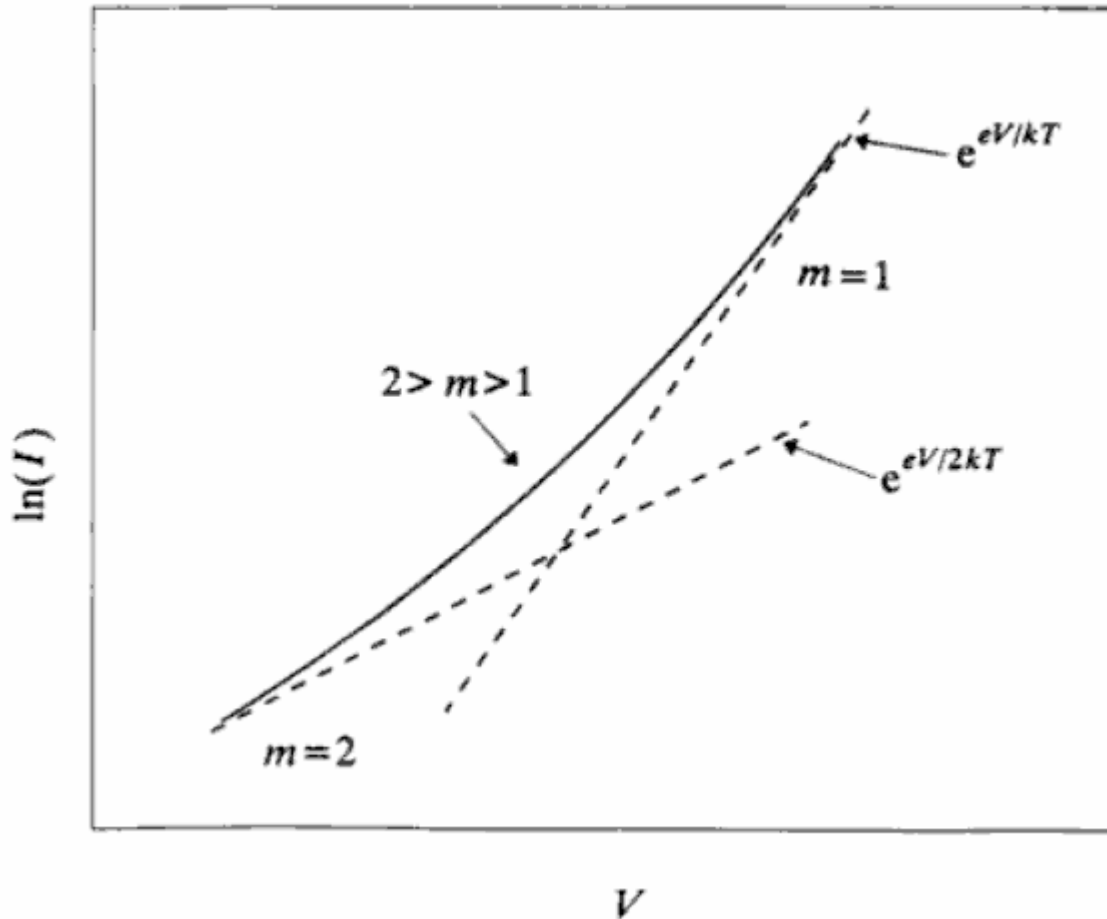


Figure 2.9. Dark I-V curve with one and two equivalent diode models

Until now the analysis has not explained the characteristics observe in many solar cells amounting to values of  $m > 2$  at low bias voltage; Apart from current leakages that can be modelled as a parallel resistance different causes have been suggested such as the tunnel effect, breakdown by microplasmas, leaks along surface channels, etc. But in the majority of practical cases, a model based on a single exponential, such as equation (2.9), or at most two, such as the sum of equations (2.7) and (2.8), is sufficient.

## 2.5. Characteristic I-V curve under illumination

According to equation (2.1), the current supplied by a solar cell to a load is that given by the difference between the photocurrent  $I_L$  and the recombination current  $I_D(V)$ , the latter being due to the bias from the generated voltage. If we assume, to simplify things, that a single exponential can express the current in the diode, the characteristic equation for the device is:

$$I = I_L - I_0 \left[ \exp\left(\frac{eV}{mkT}\right) - 1 \right] \quad (2.10)$$

The characteristic  $I$ - $V$  curve represented by this equation is drawn in the standard way in Figure 2.10.

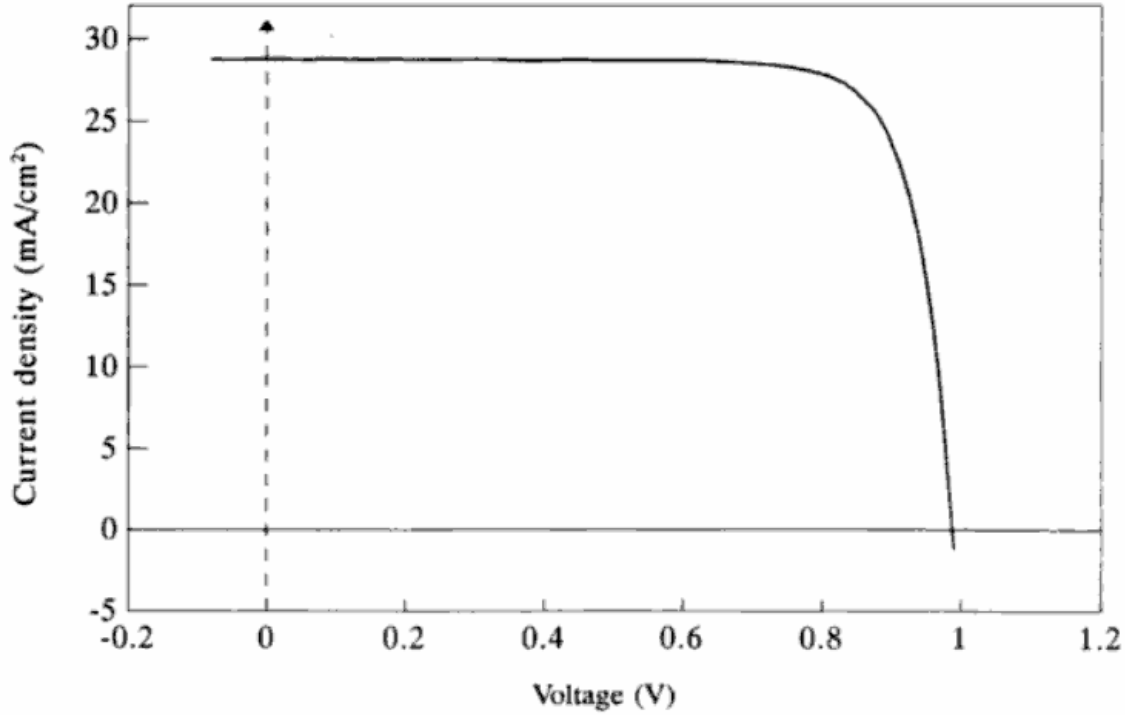


Figure 2.10. Illuminated  $I$ - $V$  curve

This way of drawing the curves adopts a sign convention that takes generated current as positive (the opposite to the convention used with diodes as normal circuit elements). By this convention, the first quadrant of the  $I$ - $V$  plane corresponds to the regime where the cell delivers current to the load to which a positive voltage is applied. In other words, the device functions as a generator of energy.

### 2.5.1. Short-circuit current and open-circuit voltage

As seen from Figure 2.10, the greatest value of current with the cell as a generator (in the first quadrant) is obtained under short-circuit conditions, when  $V = 0$ . According to equation (2.10), the short-circuit current  $I_{SC}$ , is given by:

$$I_{SC} \equiv I(V = 0) = I_L \quad (2.11)$$

If the device is kept in open-circuit, so that  $I = 0$ , it biases itself with a voltage that is the greatest that can arise in the first quadrant. This is called the open-circuit voltage  $V_{OC}$ . Its value is such that the photocurrent is completely cancelled by the bias current, that is to say  $I_L = I_D(V_{OC})$  under open-circuit conditions. Then, from equation (2.10), we find:

$$V_{OC} = m \frac{kT}{q} \ln \left[ \frac{I_L}{I_0} + 1 \right] \quad (2.12)$$

The definition of the above two operating parameters allows us to write the characteristic curve of the cell in the following alternative form:

$$I = I_{SC} \left[ 1 - \exp \left( - \frac{e(V_{OC} - V)}{mkT} \right) \right] \quad (2.13)$$

This form is sometimes useful. The formula is accurate about the open-circuit point, but its validity for the whole working range is questionable since the parameters  $m$  and  $I_0$  of equation (2.10) depend, to some extent, on the position on the curve.

### 2.5.2. Maximum-power point

The region of the curve between  $I_{OC}$  and  $V_{OC}$  corresponds to operation of the cell as a generator.

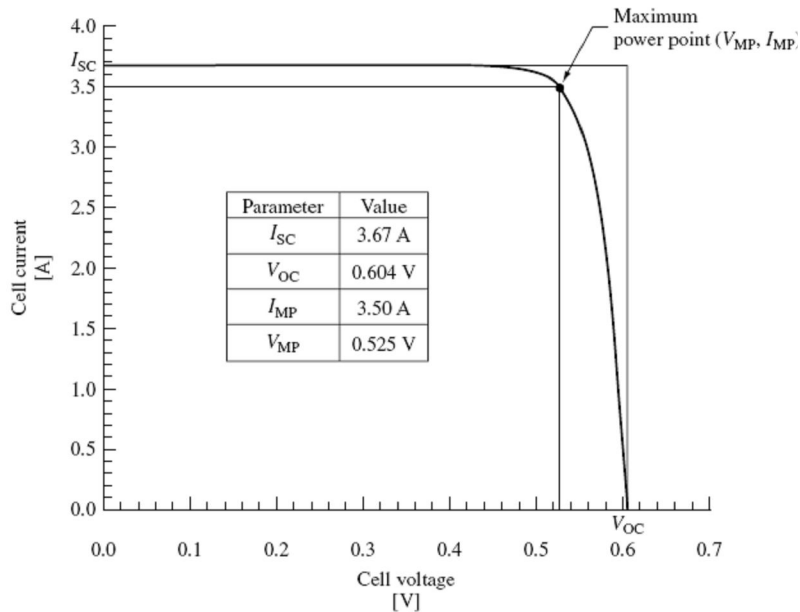


Figure 2.11. Maximum operating point

In Figure 2.11, the product  $P = IV$  gives the power supplied. There exists an operating point  $(I_M, V_M)$  at which the power dissipated in the load is maximum. This is called the maximum-power point. The values of  $I_M$  and  $V_M$  can be obtained from the usual condition for a maximum:

$$\frac{dP}{dV} = 0 \quad \text{or} \quad 0 = d(IV)_M \equiv I_M dV + V_M dI \quad (2.14)$$

which can also be written as:

$$\left[ \frac{dI}{dV} \right]_M = -\frac{I_M}{V_M} \quad (2.15)$$

This represents a completely general condition for a maximum. When it is applied to a cell described by the equation (2.10), the result is:

$$I_M = \frac{I_L + I_0}{1 + \frac{mkT}{eV_M}} \quad (2.16)$$

The characteristic equation of the cell should also be satisfied:

$$I_M = I_L - I_0 \left[ \exp \frac{eV_M}{mkT} - 1 \right] \quad (2.17)$$

From these two simultaneous equations,  $I_M$  and  $V_M$  may be calculated. However, the system has no explicit solution. It is necessary to solve transcendental equation. A very approximate analytic solution is:

$$\frac{I_M}{I_L} = 1 - a^{-b} \quad (2.18)$$

where

$$a = 1 + \ln \frac{I_L}{I_0} \quad \text{and} \quad b = \frac{a}{a+1} \quad (2.19)$$

$$\frac{V_M}{V_{OC}} \approx 1 - \frac{\ln a}{a}$$

For the usual values applicable to practical solar cells, the formulas predict values of  $I_M$  close to those of  $I_L$  and values of  $V_M$  close to those of  $V_{OC}$ . This is seen in the curves of Figure 2.12. Consequently, the maximum-power point is close to the elbow of the characteristic curve, as indicated in Figure 2.11.

### 2.5.3. Fill factor and energy conversion efficiency

The product  $I_M \cdot V_M$ , which corresponds to the maximum power that can be delivered to the load, is represented in Figure 2.11 by the area of the shaded rectangle. This is obviously smaller than the area corresponding to the product  $I_{SC} \cdot V_{OC}$  (the greatest current that can be extracted from the cell divided by the greatest voltage). The more pronounced the elbow of the characteristic curve, however, the closer the two products come to being equal. The quotient defined by:

$$FF = \frac{I_M \cdot V_M}{I_{SC} \cdot V_{OC}} \quad (2.20)$$

is nonetheless always less than one. It is called the *fill factor* and gives a quantitative measure of the form of the characteristic curve. The fill factor is a parameter of great practical value. It varies little among devices and takes values in the range 0.7 to 0.8 for many crystalline semiconductor cells (*Si, GaAs, InP, etc.*).

Making use of the definition of fill factor, we can write the maximum power delivered by the cell as:

$$P_M = FF \cdot I_{sc} \cdot V_{oc} \quad (2.21)$$

Employing expressions (2.18) and (2.19), and considering that in practical cells  $a$  is greater than 20, we can obtain the following approximate and simple formulas for  $FF$ :

$$FF = 1 - \frac{\ln a - 1}{a} \quad (2.22)$$

This formula predicts a small variation in  $FF$  depending on the cell and operating conditions. Consequently, equation (2.12) highlights the dependence of the maximum power with respect to the basic operating parameters, the short-circuit current and the open-circuit voltage.

The *energy-conversion efficiency* of a solar cell is defined as the ratio between the maximum electrical power that can be delivered to the load and the power  $P_L$  of the radiation incident on the cell:

$$\eta = \frac{I_M V_M}{P_L} \equiv \frac{FF \cdot I_{sc} V_{oc}}{PL} \quad (2.23)$$

Of course, this efficiency and the maximum power output are obtained only if the resistance of the load has the right value of  $V_M/I_M$ .

## 2.6. Equivalent circuit of a solar cell

Equation (2.10) describes analytically the behaviour of a solar cell. In practice it is generally very convenient, however, to be able to describe this same behaviour using circuit elements. This option is especially useful when it comes to considering many cells connected in series or in parallel, as occurs in a photovoltaic module.

### 2.6.1. Equivalent circuit of the ideal device

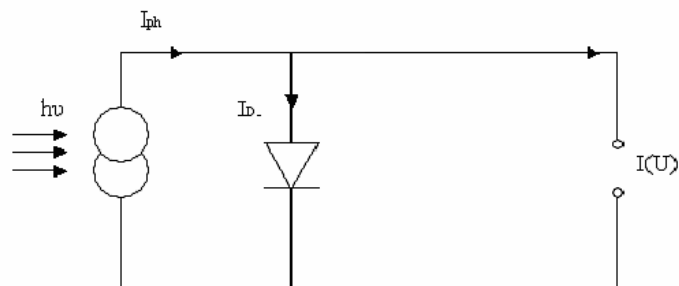
The circuit of Figure 2.12(a), consisting of an ideal  $p-n$  junction diode having saturation current  $I_0$  and ideality factor  $m$ , and of an ideal current source  $I_L$ , has the same behaviour as represented by equation (2.10). This is apparent when we consider the currents flowing into each node of the circuit. Therefore, this is the equivalent circuit of the ideal device.

## 2.6.2. Series and parallel resistances

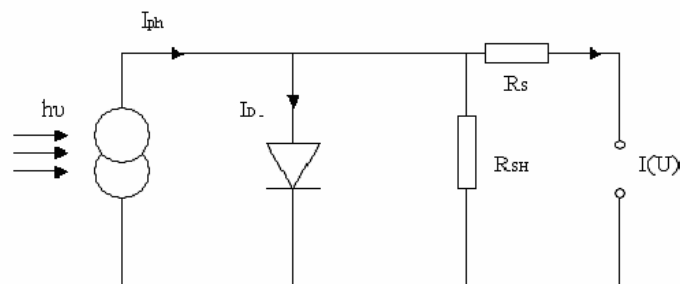
Nevertheless, in a real solar cell there exist other effects, not accounted for by equation (2.10). These affect the external behaviour of the cell. We shall consider at least two of these extrinsic effects: the series resistance and current leaks proportional to the voltage. The latter are usually characterized by a parallel resistance. These effects are distributed throughout the device and cannot always be represented by a resistance of constant value. However, from a practical and functional point of view, the use of lumped resistances to represent them — as shown in the equivalent circuit of Figure 2.12(b) — turns out to be an acceptable and extremely useful solution.

The parallel resistance has its greatest effect when the voltage is lowest, i.e. when the current passing through the diode of the equivalent circuit is very small. The origin of this resistance may be leakage around the edge of the cell, diffusion paths along dislocations or grain boundaries (when these are present), small metallic short circuits, etc. The origin and rigorous study of the parallel resistance is generally rather complex. Fortunately, though, in many practical cases (including present-day crystalline silicon solar cells) it has little importance under normal operating conditions (and even less when operated under concentrated light).

This is not so, however, with the series resistance, which is due to the resistance of the metal contacts with the semiconductor, the resistance of the layers of the semiconductor itself (in which lateral currents may flow) and to the resistance of the metallic fingers which make up the front grid of the cell.



a)



b)

Figure 2.12. Equivalent circuits of solar cells

Once  $R_S$  and  $R_{SH}$  are included, the equation for the solar cell can be written:

$$I = I_L - I_0 \left[ \exp \frac{e(V + IR_S)}{mkT} - 1 \right] - \frac{V + IR_S}{R_{SH}} \quad (2.24)$$

The above is obtained from an analysis of the equivalent circuit of Figure 2.12(b).

The effects of  $R_S$  and  $R_P$  on the extrinsic behaviour of the cell are illustrated in Figure 2.13. By studying this diagram we can confirm that the effect of parallel resistance — when it is sufficiently small — is to reduce the open-circuit voltage and the fill factor. The short-circuit current is not affected by it.

A large series resistance, on the other hand, reduces the fill factor and the short-circuit current, without affecting the open-circuit voltage. Even when the cell is in short circuit, with zero external voltage, the junction is biased by a voltage of value  $I_{SC}R_S$ , produced by the passage of current through  $R_S$ . This bias produces a current through the diode in the opposite direction to  $I_{SC}$ . The effect on  $I_{SC}$  is not, however, very marked in practical cells since correct design should limit  $R_S$  to a fairly low value. The situation is different, though, as regards the effect on fill factor. This can be degraded significantly, resulting in poor efficiency, especially if the current is high as in cells working under optical concentrators. As a practical guide we can say that the product  $I_{SC}R_S$  should not be much greater than  $kT/e$  (equal to about 25 mV, at ambient temperature).

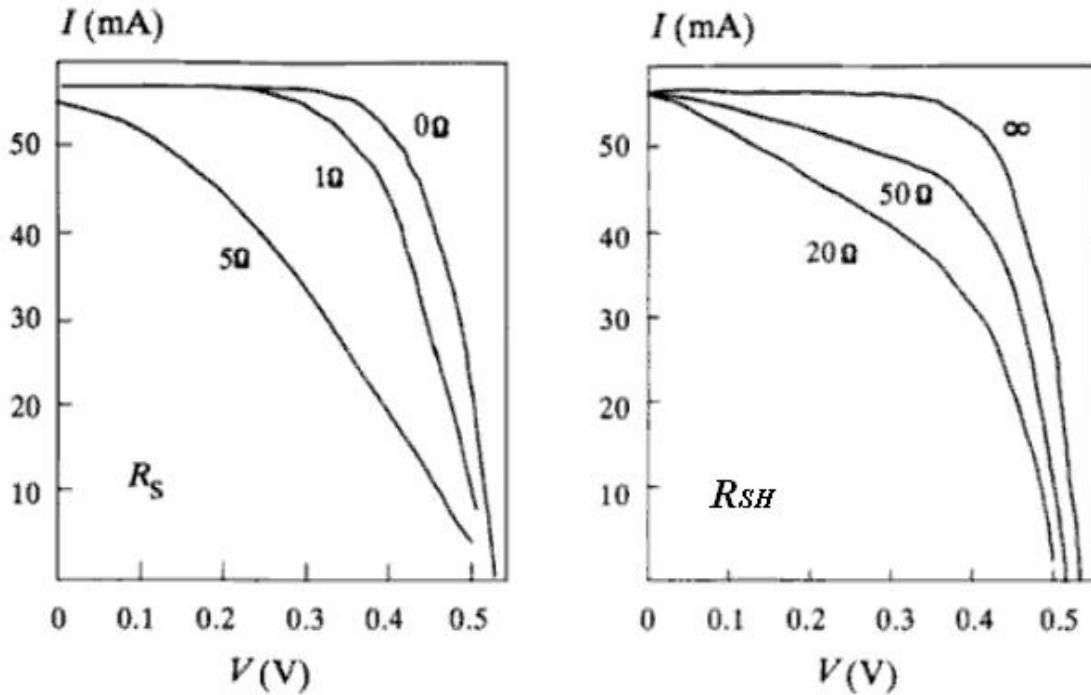


Figure 2.13. The effects of the series  $R_S$  and parallel  $R_{SH}$  on the  $I-V$  curve

A deeper explanation of the effects of series and parallel is showed in the experimental parts.

## 2.7. Variations from the basic behaviour

On the earth, variations of temperature and of the intensity of the radiation are important considerations regarding solar cells. The variations of climate throughout the year is one instance. Also, cells may be used in optical concentrators that increase the intensity of the incident light and consequently the temperature of operation.

In all the examples given, to design and use solar cells correctly it is evidently necessary to understand how the two parameters, temperature and intensity of radiation, influence their behaviour.

### 2.7.1. The effect of temperature

As an illustration of the effect of temperature, let us consider a cell described by an exponential with  $m = 1$ , corresponding to behaviour dominated by recombination currents in the neutral zones. This is adequate as a first approximation. The characteristic equation for the device is therefore:

$$I = I_L - I_0(T) \left[ \exp \frac{e(V + IR_s)}{mkT} - 1 \right] \quad (2.25)$$

The photocurrent  $I_L$  increases slightly with temperature, in part because of greater diffusion lengths of the minority carriers and in part because of the narrowing of the bandgap that displaces the absorption threshold towards photons of lower energy. This improvement of the photocurrent with temperature is more appreciable in *GaAs* than in *Si* cells. It is always quite small, however, and can be ignored as a first approximation.

Therefore, the change in the characteristic equation of the cell with temperature arises through the exponential term and through  $I_0(T)$ . The dependence of the reverse-bias saturation current on temperature can be written in the following form:

$$I_0 = kT^3 \exp \left( - \frac{E_{G0}}{kT} \right) \quad (2.26)$$

where  $k$  and  $E_{G0}$  (the bandgap at 0 K) are both approximately constant with respect to temperature.

Taking into account equations (2.25) and (2.26), we can immediately deduce the following expression for open-circuit voltage:

$$V_{oc}(T) = \frac{E_{G0}}{e} - \frac{kT}{e} \ln \left( \frac{kT^3}{I_L} \right) \quad (2.27)$$



It predicts a decrease of  $V_{OC}$  with temperature (see Figure 2.14). The importance of this variation is more readily appreciated by means of the following coefficient of variation:

$$\frac{dV_{OC}}{dT} = -\frac{1}{T} \left[ \frac{E_{G0}}{e} - V_{OC}(T) \right] \quad (2.28)$$

This takes a value of about  $-2.3 \text{ mV}/^\circ\text{C}$  for silicon cells at ambient temperature.

The fill factor also diminishes as temperature is increased. This decrease in  $FF$  is due to the increase in  $I_0$  and to the rounding of the elbow of the characteristic  $I$ - $V$  curve, evident from the effect of increasing  $T$  in the exponential term of equation (2.25).

The decrease in  $V_{OC}$  and  $FF$  with temperature more than outweighs the slight increase in  $I_L$ , and there is a marked decrease in the efficiency of a solar cell as temperature is increased. This is illustrated in Figure 2.14. At operating temperatures near to the ambient, the change is roughly 0.04 to 0.06 percent points per Celsius degree for silicon cells, and 0.012 to 0.03 percent points per degree for gallium arsenide cells.

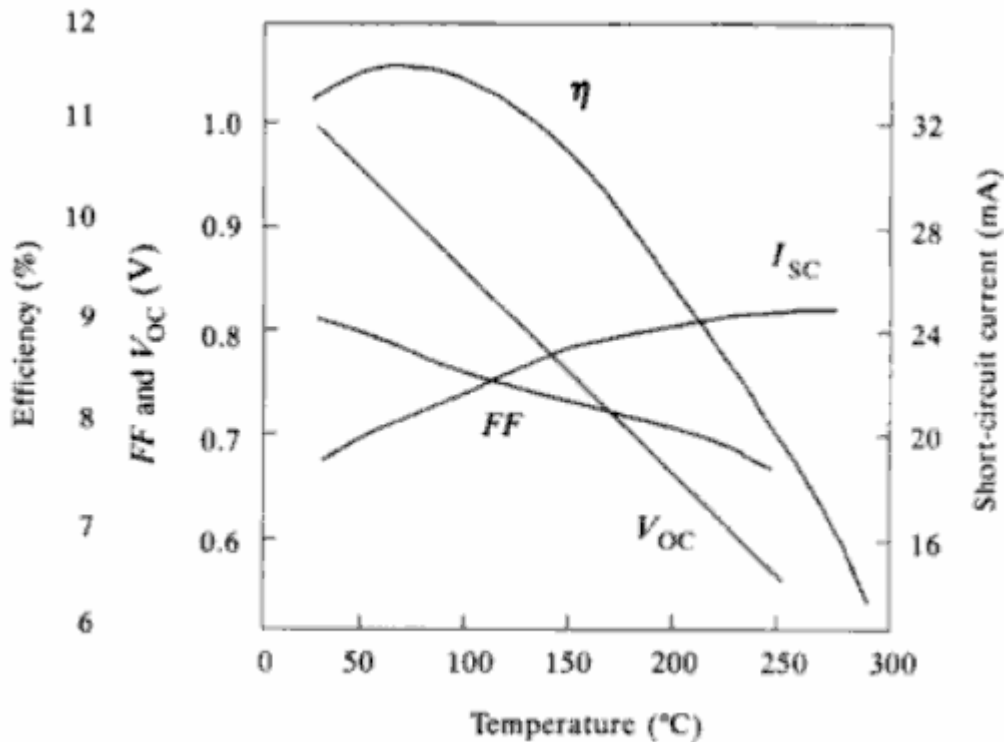


Figure 2.14. Variation of operating parameters with temperature[2]

The effects of the temperature are showing later in the experimental part.

### 2.7.2. The effect of illumination intensity

Over a wide range of operating conditions, the photocurrent of practical solar cells is directly proportional to the intensity of the incident, radiation. This proportionality makes possible the following analysis. If the photocurrent at the level of

radiation defined as unity (normally 1 sun AMI = 100 mW/cm<sup>2</sup>) is  $I_{L1}$  the photocurrent at a level of radiation  $X$  (concentration factor:  $X$  suns) times greater is:

$$I_L = XI_{L1} \quad (2.29)$$

If  $V_{OC1}$  is the open-circuit voltage at 1 sun, the voltage at  $X$  suns is obtained by application of equation (2.12), resulting in:

$$V_{OC} = V_{OC1} + \frac{mkT}{q} \ln X \quad (2.30)$$

It is assumed that  $m$  and  $I_0$  do not change appreciably as the level of illumination is increased.

The fill factor of the intrinsic cell ( $R_S = 0$  and  $R_{SH} = \infty$ ) also increases slightly with the level of illumination, as is easily deduced from equations (2.18), (2.19) and (2.22).

Consequently, the efficiency of a cell subject to an arbitrary level of illumination defined by  $P = X P_{L1}$ , is given by:

$$\eta(x) = \frac{XI_{L1}V_{OC}(x)FF(x)}{XP_{L1}} = \frac{I_{L1}V_{OC}(x)FF(x)}{P_{L1}} \quad (2.31)$$

Then, with equation (2.30) taken into account:

$$\eta(x) = \frac{I_{L1}V_{OC1}FF(x)}{P_{L1}} \left[ 1 + \frac{mkT}{eV_{OC1}} \ln X \right] \quad (2.32)$$

If we ignore small variations in  $FF$ , the above expressions predict an increase of efficiency due to the increase in open-circuit voltage. This voltage varies logarithmically with the concentration level. The increase cannot continue indefinitely, even in an ideal device, due to physical limits not apparent in the analysis until now. In practice, however, these theoretical limits do not manifest themselves at low levels of illumination and we do observe a logarithmic increase in efficiency. But if the intensity of illumination, and hence the photogenerated current, is increased further, the ohmic losses due to the series resistance of the cell are no longer negligible and become responsible for a considerable deterioration in the efficiency of the device.

As a net result of all the factors mentioned, the variation in energy-conversion efficiency of a solar cell with the illumination intensity typically has the form shown in Figure 2.15.

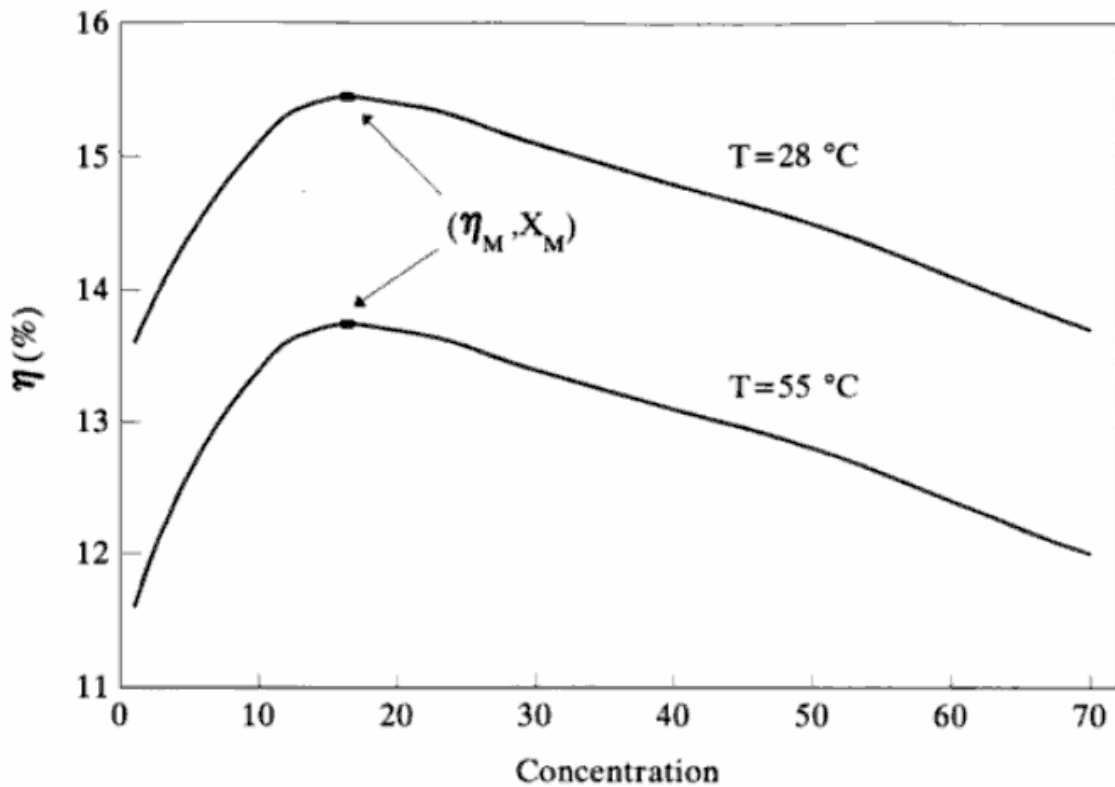


Figure 2.15. Variation of the conversion efficiency with the concentration of the light.[2]

In the curve of Figure 2.15, three distinct regions can be seen: (a) low concentrations, where the effect of series resistance is negligible and the curve is almost ideal, giving a logarithmic growth with  $X$ ; (b) high concentrations, where series-resistance effects dominate, and efficiency falls off rapidly with the concentration and (c) intermediate concentrations, where both tendencies counteract, and there is a slow variation in efficiency around the maximum.

The form of the characteristic  $\eta$ - $X$  curve of Figure 2.15 makes evident the great importance of the series resistance in the design of solar cells. The design is influenced considerably in this respect by the levels of concentration at which the device operates.

## 3. Experimental

### 3.1. Dark I-V measurements of solar cells.

#### 3.1.1. Introduction

The current voltage characteristics of photocells, determined under illumination as well as in the dark, represent a very valuable tool for characterizing the electronic properties of solar cells.

Particularly denominating the dark characteristics is the easy way to estimate the quality of the junction, antireflection layers, grid and contact resistances. The usual equations (recombination and diffusion current) cannot fit some cells, and the trap-assisted tunnelling current and field-assisted recombination should be added to the two-exponential model. For the recombination, the temperature dependence is greater than that for the trap-assisted tunnelling.

The series and shunt resistance of the cell influence the fill factor ( $FF$ ), the maximum power ( $P_M$ ) and the efficiency of the cell ( $\eta$ ). In a good silicon solar cell, the series resistance ( $R_S$ ) will be less than  $0.5\Omega$ , and the shunt resistance  $R_{SH}$  will be at least  $500\Omega$ . [4]

It has been assumed that the  $I-V$  curve under illumination can be described as a superposition of dark  $I-V$  current and a voltage independent photocurrent.

The principal power losses in a solar cell are associated with the light absorption and recombination processes of the charge carriers. The diffusion effects in the junction region and electron-holes recombination are limiting the fill factor  $FF$ , so the  $FF$  value determines the maximum power point position. The fill factor decrease with temperature increase, caused by  $R_S$  and  $R_{SH}$  of the solar cell, which can be deduced from the  $I-V$  dark characteristic.

The effect of the series resistance  $R_S$  on the fill factor can be described by:

$$FF = FF_0 \left( 1 - \frac{R_S I_{sc}}{V_{oc}} \right) \quad (3.1)$$

Where  $FF_0$  is the ideal fill factor. There is also a strong relationship between the shunt resistance and the fill factor, namely the larger  $R_{SH}$  the larger is the fill factor. For one solar cell type, the larger shunt resistance and smaller series resistance go together with a higher efficiency of the solar cells.

First supposition: One diode equivalent model.

This means that an infinite value of the shunt resistance is taken. It can be estimate the value of the series resistance  $R_S$  from the semi-logarithmic plot  $I$ - $V$  from the equation:

$$I = I_s \exp\left[\frac{e(V - IR_S)}{mkT}\right] \quad (3.2)$$

The effect of recombination in the depletion region can be deduced from the dark  $I$ - $V$  characteristic for low currents. The value of the recombination currents is dependent on the concentration of generation-recombination centres. These centres could be constituted from the various impurities and defects of the grid. For high currents the series resistance  $R_S$  should be taken into account. It could be estimated from the slope on the semi-logarithmic plot on the basis of the last equation.

This result indicates that the series resistance influences the characteristic only in the region of high currents, at current  $I'$  and voltage  $\Delta V = I'R_S$ , making a deviation from the ideal characteristic.

To estimate  $R_S$  is enough to solve the last equation:

$$\begin{aligned} I &= I_s \exp\left[\frac{e(V - IR_S)}{mkT}\right] \\ \ln I &= \ln I_s + \frac{e}{mkT}(V - IR_S) \\ R_S &= \frac{V - \left[\frac{mkT(\ln I - \ln I_s)}{e}\right]}{I} \end{aligned} \quad (3.3)$$

The series resistance can be determined directly from the measured  $I$ - $V$  characteristic with the use of the two-diode equivalent model as we can see in the second supposition.

Second supposition: Two-diode equivalent model.

The two diode equivalent model is presented in the next figure, where  $I_{D1}$  is the diffusion current,  $I_{D2}$  is the recombination current,  $I$  is the current through an applied load and  $V$  is the voltage drop across this load. The current generator on the left side of the circuit represents the photocurrent  $I_{ph}$  generated by the solar cell.

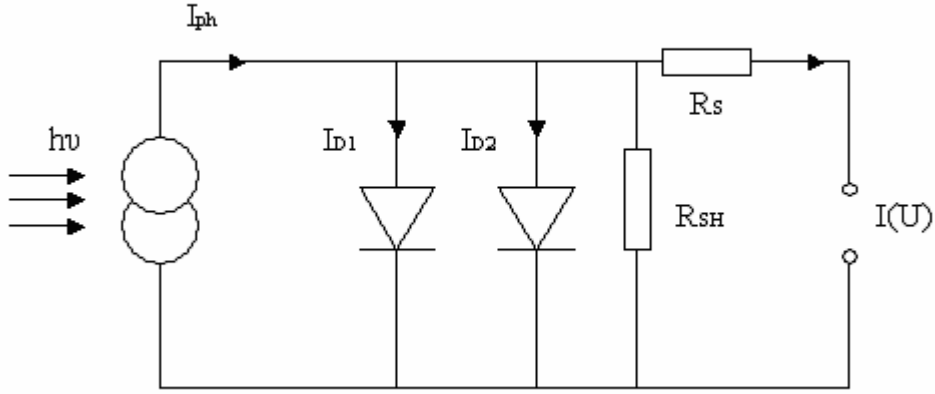


Figure 3.1: Two diode equivalent model.

The equivalent circuit has two resistors: the resistor  $R_S$  represents the series resistance in the top surface of the semiconductor and the metal contact-to-semiconductor interface and  $R_{SH}$  represents the leakage across the  $p$ - $n$  junction around the edge of the cell, and the presence of crystal defects or impurities in the junction region.[14]

The generated current can be expressed as a function of the voltage  $V$ :

$$I = I_{ph} - I_{S1} \left( \exp \frac{e(V + IR_S)}{m_1 kT} - 1 \right) - I_{S2} \left( \exp \frac{e(V + IR_S)}{m_2 kT} - 1 \right) - \frac{V + IR_S}{R_{SH}} \quad (3.4)$$

where  $I_{ph}$  is the photogenerated current,  $I_{S1}$  and  $I_{S2}$  are the diode saturation currents,  $m_1$  and  $m_2$  are ideality factors. And in dark conditions:[5]

$$I = I_{S1} \left( \exp \frac{e(V - IR_S)}{m_1 kT} \right) + I_{S2} \left( \exp \frac{e(V - IR_S)}{m_2 kT} \right) + \frac{V - IR_S}{R_{SH}} \quad (3.5)$$

The effects of the second diode and the series and parallel resistances on the  $I$ - $V$  characteristic are presented in the figure 3.2.

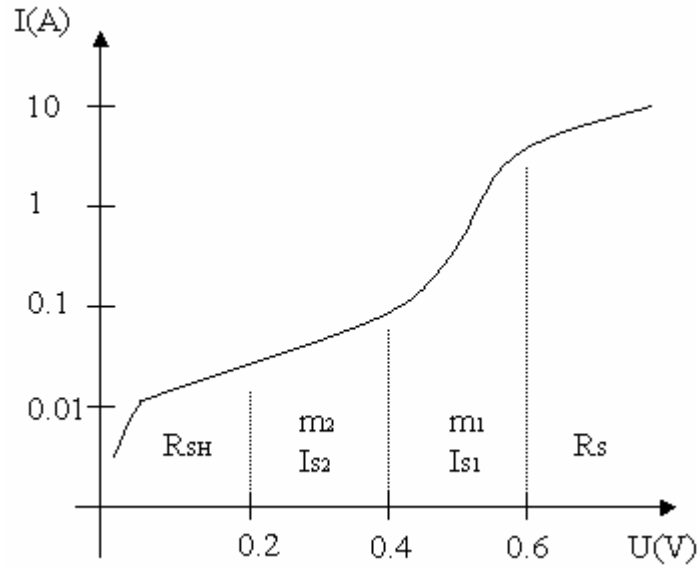


Figure 3.2. Semi-logarithmic plot of dark I-U characteristics of solar cell in the dark with the different two diode equivalent model parameters that influence the curve in the various regions.

The diffusion current is influenced by the properties of the quasi-neutral regions of the  $p-n$  junction, while the recombination mechanism are influenced by the density of defects states in the energy band gap. These second defects are formed by the energy released from recombination of electron-hole pairs.

According to diffusion theory, based on minority carrier diffusion, the value of  $m_2=1$  is associated with a next-to-ideal junction. Taking into account generation-recombination in the space charge region of the  $p-n$  junction and assuming that the energy level recombination traps are located at intrinsic Fermi level, this ideality factor should equal 2 rather than 1.[4]

In the case of solar cells, the recombination mechanism dominates over the diffusion one for low currents, while for high currents, the diffusion mechanism is significant. For small values of  $R_s$ , the product  $IR_s$  is small in comparison to  $V$ , and for low currents, the following approximation could be assumed:

$$I = I_{s1} \left( \exp \frac{e(U)}{m_1 kT} - 1 \right) + I_{s2} \left( \exp \frac{e(U)}{m_2 kT} - 1 \right) + \frac{U}{R_{SH}} \quad (3.6)$$

### 3.1.2. Experimental details.

#### 3.1.2.1. Samples

Samples C and D:

Solar cell samples have been manufactured from the low resistivity (0.4 - 0.5  $\Omega$ .cm) p-type, boron doped crystalline silicon substrates. Potential increase of the cell current by minimizing the reflection losses is done by “fine” alkaline texturization process having the theoretical optimal pyramid size for concentrator cells of 2-3 micrometers. Design of the n+ layer has to take into account the final finger spacing and current density generated by the future cell. As a result of the lateral current flowing through the n+ layer we can calculate the minimum sheet resistivity for given power losses. The samples of the cell were originally made with the area 10x10 cm. The measurements were performed on cuts of 1 quarter.

Antireflection coating was done by LP CVD deposition of the 75 nm thick silicon nitride  $\text{Si}_3\text{N}_4$  layer at the temperature about 800 °C. Design of the front side contact has been calculated for specific purposes (also specific level of illumination). Standard photolithography process has been used as an etching mask for removing silicon nitride film from the places of future metallization.

Both front and back sides metallization of concentrator solar cells are prepared by magnetron sputtering of Ti/Cu double layer (different thickness of each layer for front and back side) which are (after lift-off technique) then thickened by electroplating process in copper and tin baths. The back side field is formed (before sputtering) by Al/Si alloy from aluminum paste.

Samples A and B: The main difference with samples C and D is the front side contact. In A and B samples it have been done for bigger currents.

Sample E is like A and B samples but with 10x10 cm area.

Samples G and F are the only two non-concentrated cells that have been studied. Sample F is 10x10 cm area and G is a quarter of it.

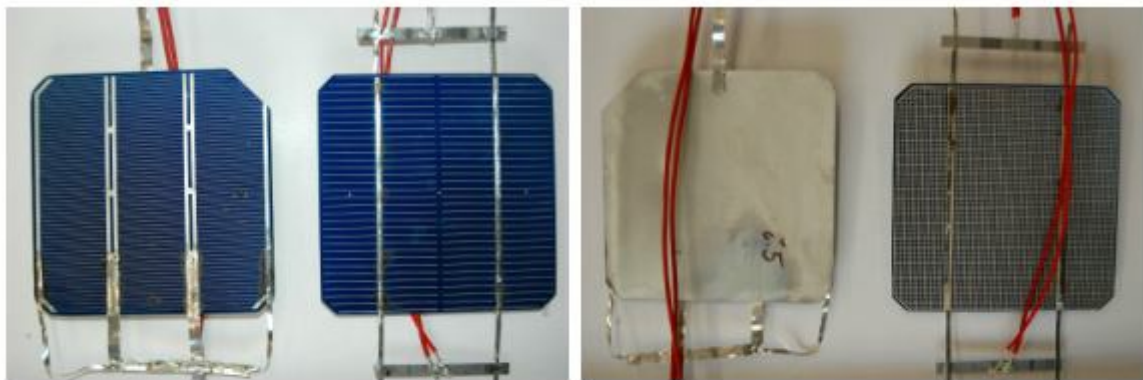




a)

b)

Figure 3.3. : a) Solar cells' C, G (non-concentrated), and A front sides respectively. b) Solar cells' C, G (non-concentrated), and A back sides respectively.



a)

b)

Figure 3.4. : a) Solar cells' E and F (non-concentrated) front sides respectively. b) Solar cells' E and F (non-concentrated) back sides respectively.

### 3.1.2.2. Connections for DC measurements.

The system for measurement that has been used is the following figures’.

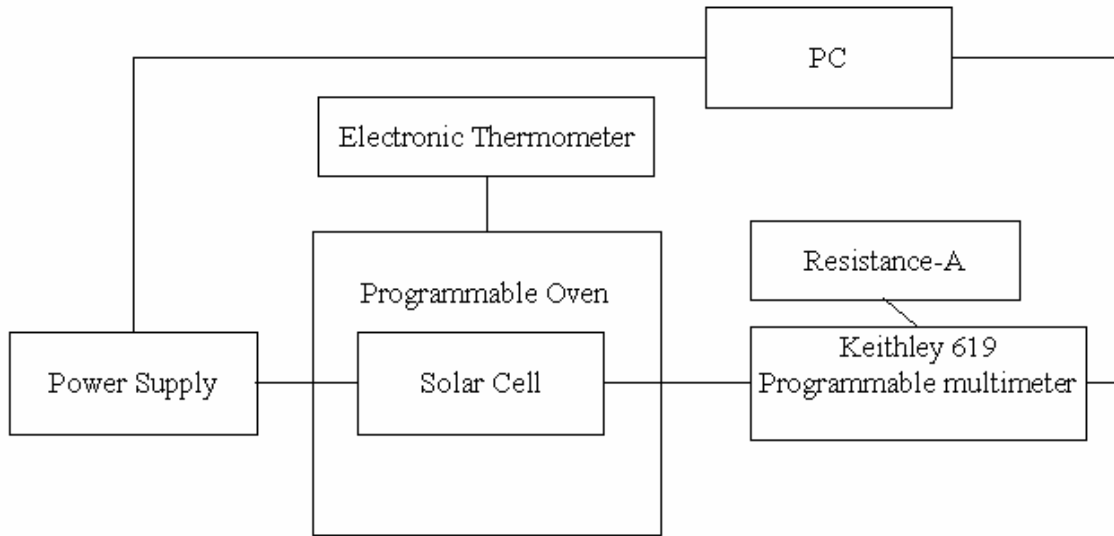


Figure 3.5: DC measurement connections.

The solar cells have been measured in dark conditions inside a programmable oven for temperatures ranging from 22°C to 77°C. A program had been developed to set the applied voltage from 0 to 0.8 (as a protection for high currents) in the sample.

Programmable power supply applies the whole circuit voltage and measures this voltage too. Programmable multimeter measures the voltage in the solar cell in the channel A and the voltage in the *Resistance-A* in the channel B. *Resistance-A* is a calibrated resistance (with value of 1.079Ω), so dividing the channel Bs’ measured voltage by the calibrated value of the resistance the current through the solar cell is measured.

The communication between PC and programmable devices had been done with the IEEE 488 standard bus. Also, the four wires method have been used, two wires to apply the signal and other two to measure without introducing significant changes on the results. Each cell measurement took about 2 minutes and other 20 minutes to stabilize the oven for each temperature.

### 3.1.3. Results.

The figure 3.4 illustrates the dark  $I$ - $V$  curve of solar cell sample B at different temperatures. As temperature grows the voltage for the same current is going down, or writing it in other words, the efficiency of the solar cell is going down.

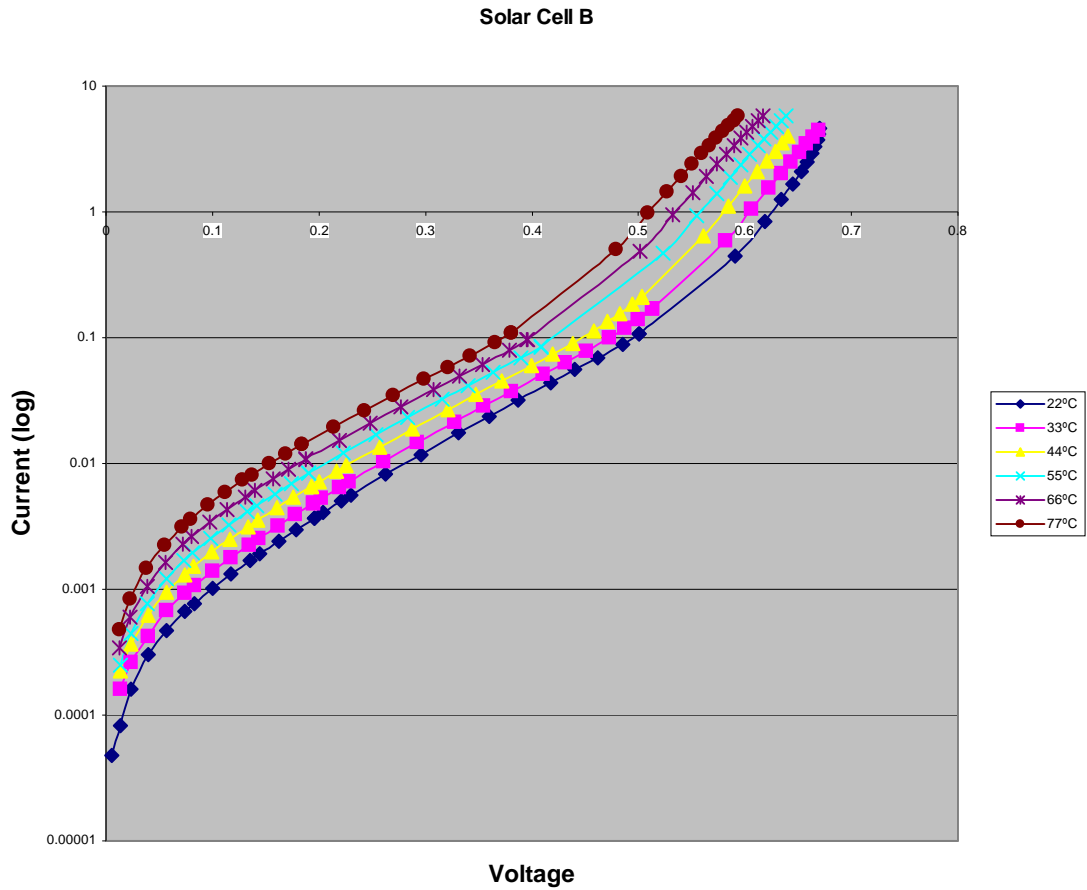


Figure 3.6: Solar Cell B's dark  $I$ - $V$  curves for all the temperature range

In the non concentrated cells the effect of the temperature appears too, but at different values as can we can see in the Figure 3.7. Lower efficiency is shown. For example, at 77°C, the sample B's voltage for 0.1 ampere current is about 0.36 volts, and in the sample G the voltage for the same current is close to 0.3 volts.

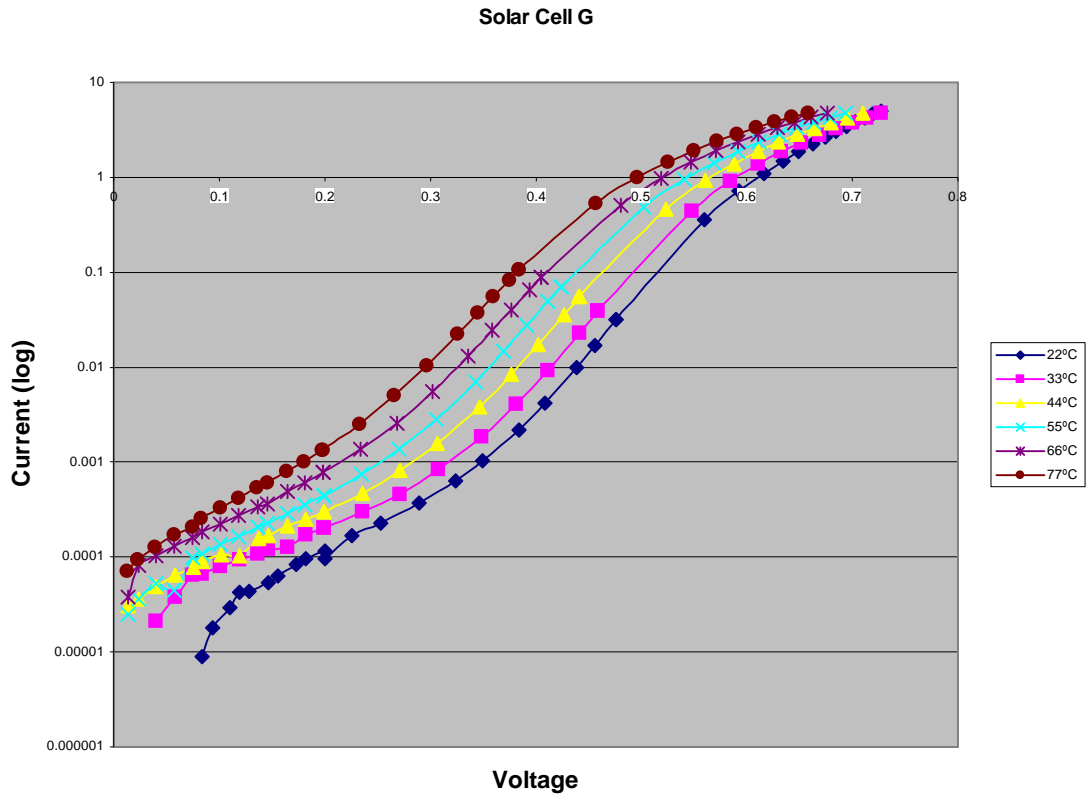


Figure 3.7: Solar Cell G dark  $I$ - $V$  curves for all the temperature range

In the next text the different ways to analyze the dark  $I$ - $V$  curves are presented. Two curves are taken to show how to get the properties of the solar cells. The concentrated solar cell C and non-concentrated solar cell G at the same temperature of 44°C.

Looking for equivalent parameters in the solar cell C at 44°C

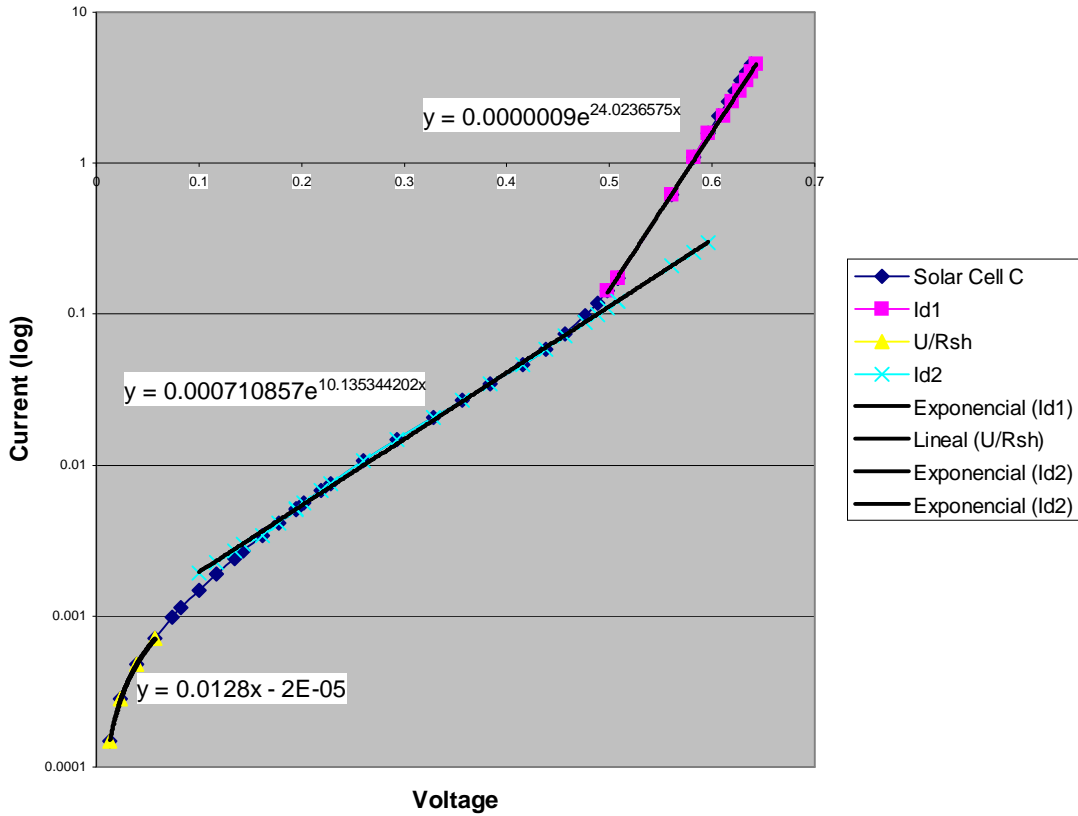


Figure 3.8: Solar Cell C dark  $I$ - $V$  curve with approximation curves

Then the method used to evaluate the electrical DC parameters is presented. The dark  $I$ - $V$  curve obtained from the measurements has been divided into the four zones of the two diode model before described.  $R_{SH}$  influence zone, second diode zone, first diode zone and  $R_S$  influence zone.

Excel's equivalent equations tool have been used taking points for each described zone as we can see in the Figure 3.8 and Figure 3.9. For each zone the calculations are presented as follows.

The equation of diode 1 model is:

$$I_{D1} = I_{S1} \exp\left(\frac{eU}{m_1 kT}\right) \quad (3.6)$$

where,

$$e = 1.62 \cdot 10^{-19} \text{ C}$$

$$k = 1.380 \ 6504 \cdot 10^{-23} \text{ J / K}$$

$$T = \text{Temperature in Kelvins} = 273.15 + T_C$$

so, the values of  $I_{S1}$  and  $m_1$  are:

$$I_{S1} = 9 \cdot 10^{-7}$$

$$\frac{e}{m_1 kT} = 24.0236575 \rightarrow m_1 = \frac{e}{24.0236575 kT} = 1.52099$$

Solving in the same way the equation of diode 2:

$$I_{D2} = I_{S2} \cdot \exp\left(\frac{eU}{m_2 kT}\right)$$

$$I_{S2} = 0.000710857 \tag{3.7}$$

$$\frac{e}{m_2 kT} = 10.135344202 \rightarrow m_2 = \frac{e}{10.135344202 kT} = 3.605353$$

For the measurement of the  $R_{SH}$  the following linear equation had been used in low current and voltage region. The slope of this equation is the influence of  $R_{SH}$  in this region.

$$I_{DARK} = \frac{U}{R_{SH}} \tag{3.8}$$

$$I_{DARK} = 0.0128 \cdot U \rightarrow R_{SH} = \frac{1}{0.0128} = 78.125 \Omega$$

In this case the calculation of  $R_S$  is not possible because of the power supply's 6 amperes output limit, which makes impossible to see the influence of the series resistance in the cell's behaviour.

In the non-concentrated G solar cell's dark  $I$ - $V$  curve had been worked in the same way as in the solar cell C.

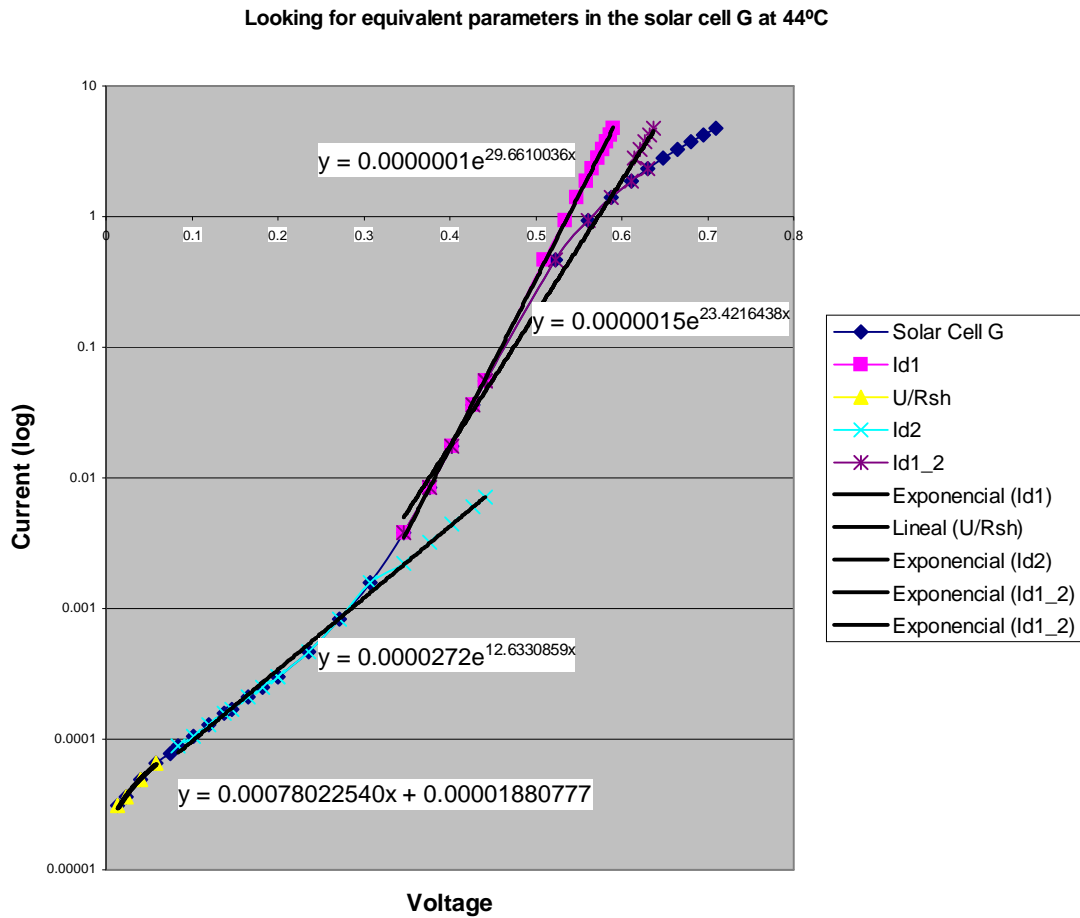


Figure 3.9: Solar Cell G dark  $I$ - $V$  curve with approximation curves

Taking in consideration the two diodes model, exponential equations are described using the points of the  $I$ - $V$  curve.

Two possible equations had been studied for the same diode 1 of two diode model equation (3.6).

The values of  $I_{S1}$  and  $m_1$  are:

$$I_{S1} = 0.0000001$$

$$\frac{e}{m_1 k T} = 29.6610036 \rightarrow m_1 = 1.231939$$

And taking  $I_{D1_2}$ , the values of saturation current  $I_{S1_2}$  and the diode ideality factor  $m_{1_2}$  are:

$$I_{S1\_2} = 0.0000015$$

$$\frac{e}{m_{1\_2}kT} = 23.4216438 \rightarrow m_{1\_2} = 1.560106$$

The  $R_S$  calculation for both  $I_{D1-s}$  ( $I_{D1}$  and  $I_{D1\_2}$ ) have been made dividing the difference between the real voltage value of the solar cell curve ( $V$ ) and voltage of the  $I_D$  curve ( $V'$ ) at the same current.

$$\Delta V = I \cdot R_S \rightarrow R_{S(I')} = \frac{\Delta V}{I'} \quad (3.9)$$

Equation 3.9 gives the  $R_{S(I')}$  for each taken high current( $I'$ ).

To just take one unique  $R_S$  value the slope of  $\Delta V$  vs.  $I$  is taken.

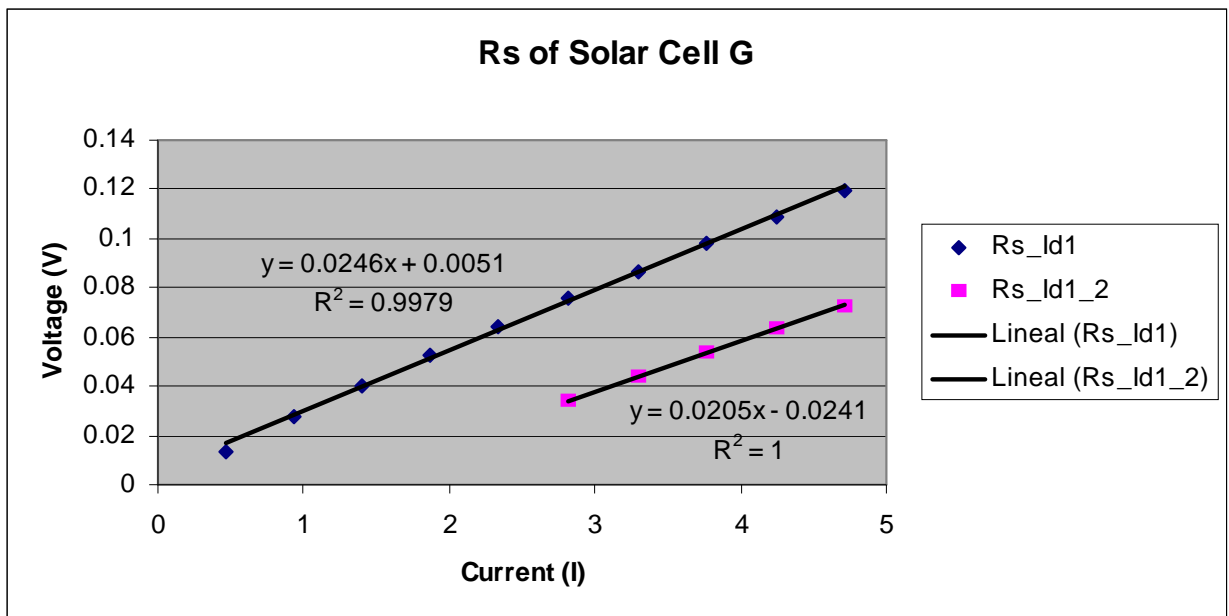


Figure 3.10:  $\Delta V$  vs. Current at high current values of Solar Cell G

The values for both cases are:

$$R_{S1} = 0.0246\Omega$$

$$R_{S1\_2} = 0.0205\Omega$$

As Figure 3.11 shows  $R_S$  value increases when temperature increases and this means bigger power losses in the solar cell.



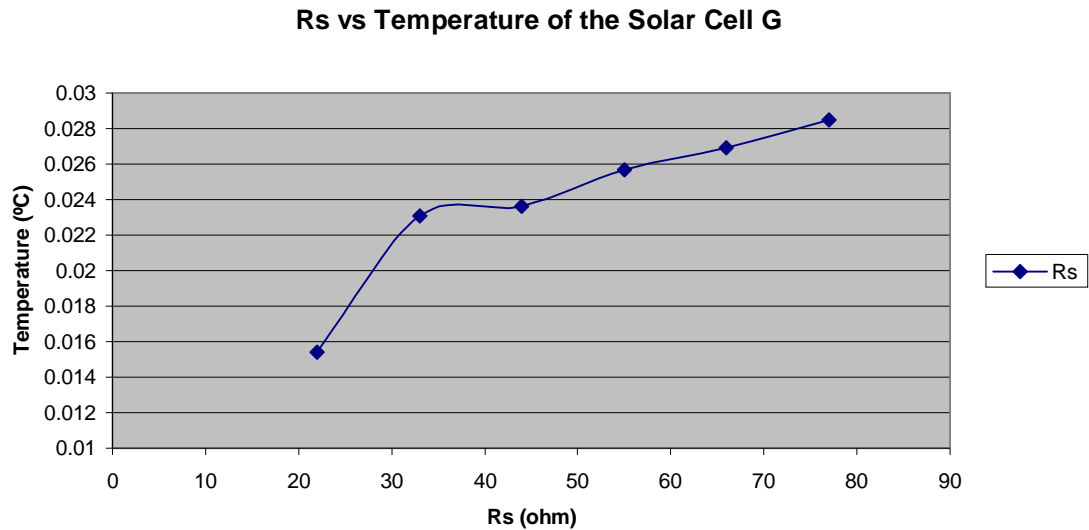


Figure 3.11 Temperature effect in  $R_S$  parameter

To obtain the parameters of the second diode of the two diode model (equation 3.7), it's done in the same before described:

$$I_{S2} = 2.72 \cdot 10^{-5}$$

$$\frac{e}{m_2 k T} = 12.6330859 \rightarrow m_2 = \frac{e}{12.6330859 k T} = 2.892425$$

For the measurement of the  $R_{SH}$  the linear equation 3.8 had been used in low current and voltage region. The slope of equation 3.8 is the influence of  $R_{SH}$  in this region, but more points at lower current are needed to estimate better this value.

$$I_{DARK} = 0.00078022540 \cdot U \rightarrow R_{SH} = \frac{1}{0.00078022540} = 1281.681 \Omega$$

## 3.2. Measurement of solar cells AC parameters

### 3.2.1. Introduction

Photovoltaic cells are operated as DC devices. But they exhibit a complex impedance due to the solar cell design. Subsequent electronic circuits for electric power conditioning are designed to match the input at standard operating conditions. During operating the real part as well as the imaginary part of the impedance of photovoltaic cells change due to ambient conditions such as illumination and temperature. A mismatch due to changes of the complex impedance can lead to a reduced performance of the whole generating system. Hence, for designing such efficient high power photovoltaic systems detailed study on AC parameters of solar cells is important. To study the potential effect of temperature on system performance, the AC parameters of solar cells are determined at different temperatures using AC small signal measurement techniques. The cell transition capacitance and the cell conductance are calculated from small signal impedance under dark condition. It is observed that the solar cell capacitance increases whereas the real part of cell impedance decreases with temperature increasing. [6]

Complex impedance:

Analysis of the behaviour of PV devices supplying AC signal on dark conditions has been developed to easily and quickly evaluate some parameters (like the series and shunt resistances and capacitance) affecting their electrical characteristics.[7]

Circuit model.

Therefore, to monitor the different parameters, it can be interesting to consider the solar cell as an equivalent electrical circuit, based on a parallel of a capacitance and a resistance, series connected to another resistance, and to investigate its behaviour on dark condition under an AC signal.

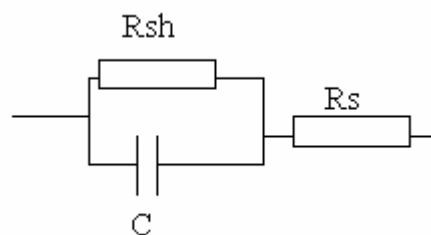


Figure 3.12 : Solar cell AC equivalent circuit

The analysis of the circuit complex impedance and the comparison between its real and the imaginary parts, by means of the Nyquist diagram, allows to estimate the values of the electrical circuit main components. In fact it can be easy to show that the Nyquist diagram of such an equivalent circuit results exactly into a semi-circumference.

Firstly, let's have a circuit consisting of a capacitance  $C$  parallel connected to a resistance  $R_{SH}$ ; the equivalent admittance is the sum of the single ones:

$$\begin{aligned}
Y &= Y_1 + Y_2 \\
Y_1 &= 1/R_{SH} \quad \text{and} \quad Y_2 = j\omega C \\
Y &= 1/R_{SH} + j\omega C = (1 + j\omega CR_{SH})/R_{SH} \quad (3.10) \\
\text{impedance } Z &= 1/Y \quad \text{is} \\
Z &= R_{SH}/(1 + j\omega CR_{SH})
\end{aligned}$$

after some adjustments in the last equation:

$$Z = R_{SH}/(1 + \omega^2 C^2 R_{SH}^2) - j\omega CR_{SH}^2/(1 + \omega^2 C^2 R_{SH}^2) \quad (3.11)$$

putting

$$\begin{aligned}
R &= R_{SH}/(1 + \omega^2 C^2 R_{SH}^2) \\
X &= \omega CR_{SH}^2/(1 + \omega^2 C^2 R_{SH}^2)
\end{aligned} \quad (3.12) \quad (3.13)$$

and dividing (3.12) by (3.13) the following equation is obtained:

$$\begin{aligned}
R &= R_{SH}/(1 + X^2/R^2) \\
\text{or } R^2 + X^2 - RR_{SH} &= 0
\end{aligned} \quad (3.14)$$

Last equation is a semi-circumference with radius  $R_{SH}/2$  passing through the origin. Connecting  $R_S$  the equation becomes:

$$R^2 + X^2 - R(R_{SH} + 2R_S) + R_S^2 + R_S R_{SH} = 0 \quad (3.15)$$

and it is again the equation of a circumference with centre on the X-axis at the abscissa  $= R_S + R_{SH}/2$  and the radius  $R_{SH}/2$ .

By means of the Nyquist plot it is very easy to calculate the values of the main parameters of the equivalent circuit; the resistances are the intersections of the curve with the X axis and the capacitance value is given by the maximum of the reactance occurring at the frequency  $\omega = 1/CR_{SH}$ .

### 3.2.2. Experimental details.

#### 3.2.2.1. Samples.

Information about the measured samples is in chapter 3.1.2.1.

#### 3.2.2.2. Connections for AC measurements.

The system for measurement that has been used is presented in Figure 3.14.

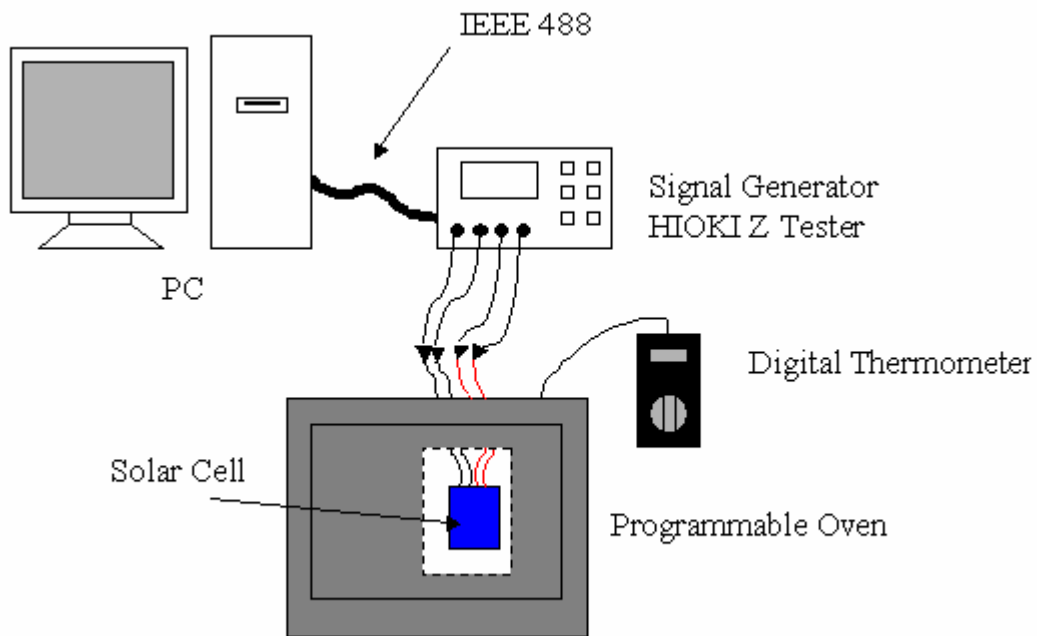


Figure 3.13 : AC measurement connections

The solar cells have been measured in dark conditions inside a programmable oven for temperatures ranging from 22°C to 77°C. A program had been used to set a sinusoidal signal at 0.05 V from 42 Hz to 130 kHz frequency range with the IEEE 488 communication between PC and signal generator. Also, the four wires method have been used, two wires to apply the signal and other two to measure without introducing significant changes on the results. Each cell measurement took about 7 minutes and other 20 minutes to stabilize the oven for each temperature.

### 3.2.3. Results.

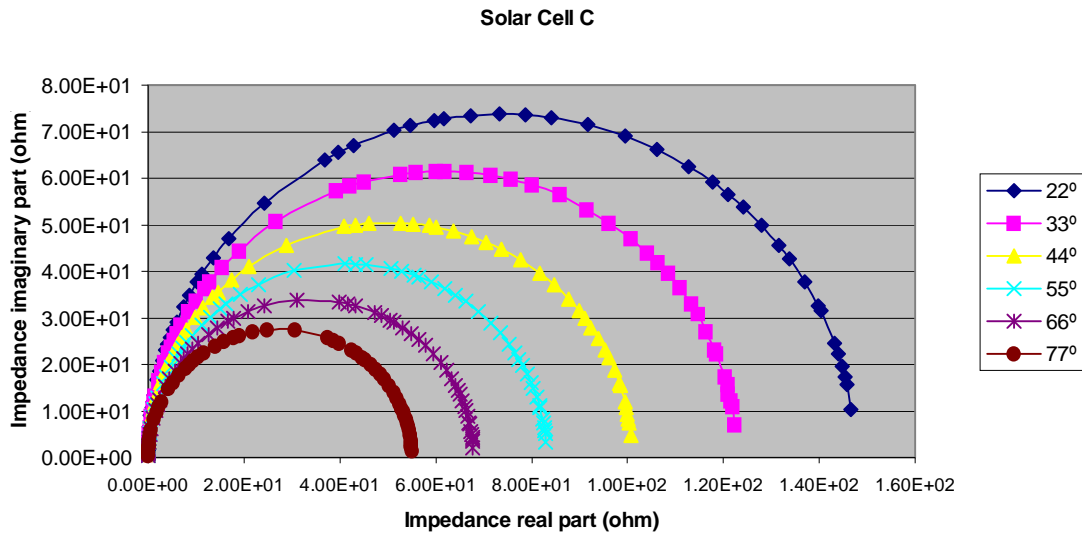


Figure 3.14: Niquist plot for single solar cell C at different temperatures.

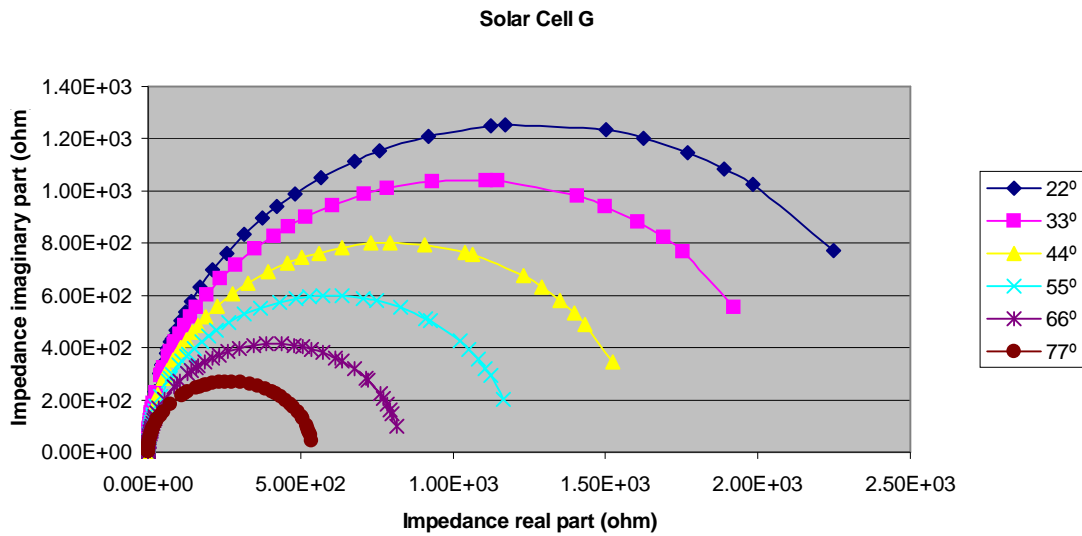


Figure 3.15: Niquist plot for single solar cell G at different temperatures.

Once all the dates had been taken for all the temperatures, like in the two figures before, a Matlab program had been used to determinate the values of the parameters following the equations that had been described before and as it is represented in the next plot.

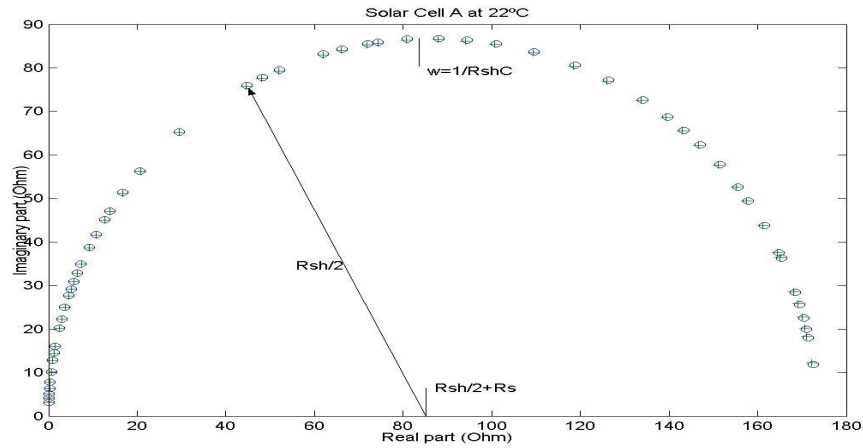


Figure 3.16: Nquist plot for the solar cell A impedances at 22°C showing how to evaluate series and shunt resistance and the capacitance of the electric equivalent circuit.

It has been used the same method with all the samples at all the temperatures. Calculation of  $R_s$  using AC method makes a big mistakes because of the high range of the high impedance range (0 to 2500  $\Omega$  in some cases).

Taking for example the concentrated cell C and the non-concentrated cell G the results are:

Solar cell C:

Temperature (°C)	$R_s$ (Ohm)	$R_{sh}$ (Ohm)	$C$ (F)
22	2.55E-04	1.47E+02	1.88E-06
33	1.27E-03	1.22E+02	1.90E-06
44	5.01E-04	1.00E+02	1.92E-06
55	1.43E-03	8.28E+01	1.94E-06
66	6.68E-04	6.74E+01	1.96E-06
77	8.91E-04	5.47E+01	1.99E-06

Figure 3.17: Values of different parameters for each measured temperature.

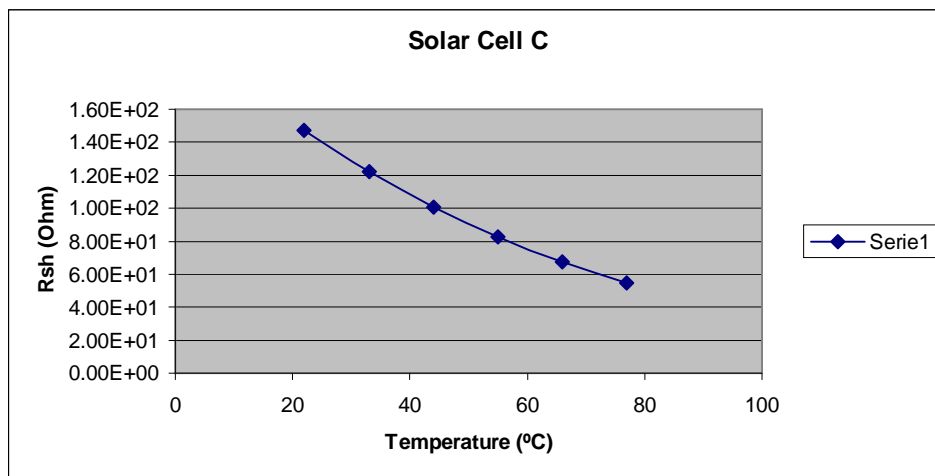


Figure 3.18 : Effect of the temperature in solar cell C's shunt resistance.

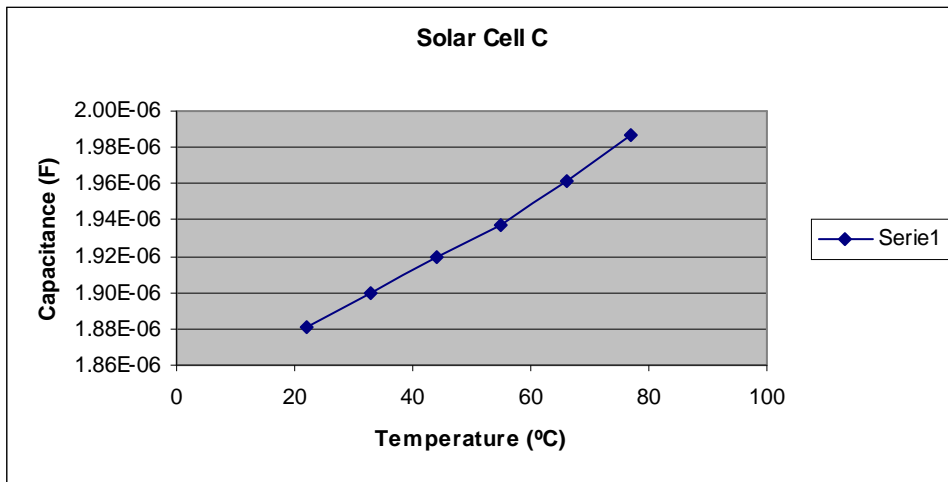


Figure 3.19: Effect of the temperature in solar cell C's capacitance.

Solar cell G:

Temperature (°C)	Rs (Ohm)	Rsh (Ohm)	C (F)
22	5.00E-02	2.51E+03	5.21E-07
33	5.11E-02	2.09E+03	5.31E-07
44	5.54E-02	1.60E+03	5.43E-07
55	5.76E-02	1.20E+03	5.55E-07
66	5.55E-02	8.27E+02	5.68E-07
77	5.77E-02	5.40E+02	5.82E-07

Figure 3.20: Values of different parameters for each measured temperature.

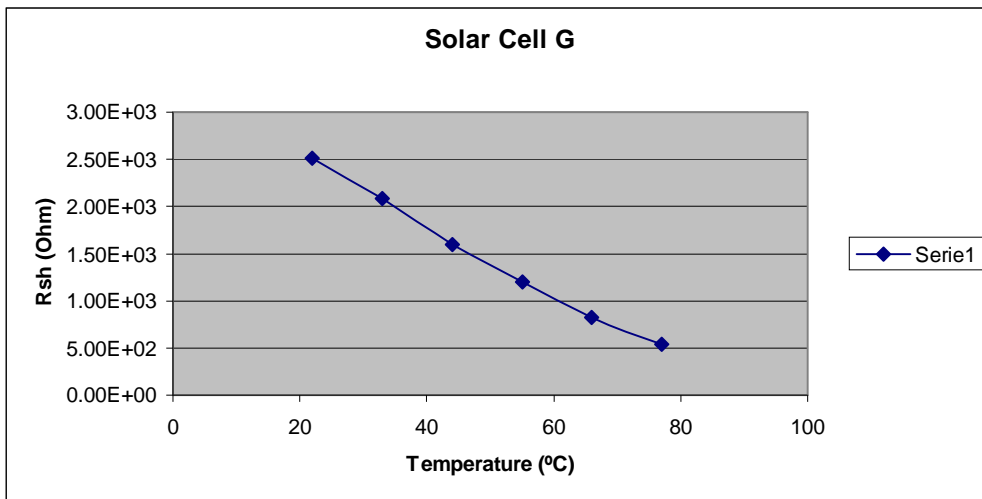


Figure 3.21: Effect of the temperature in solar cell C's shunt resistance.

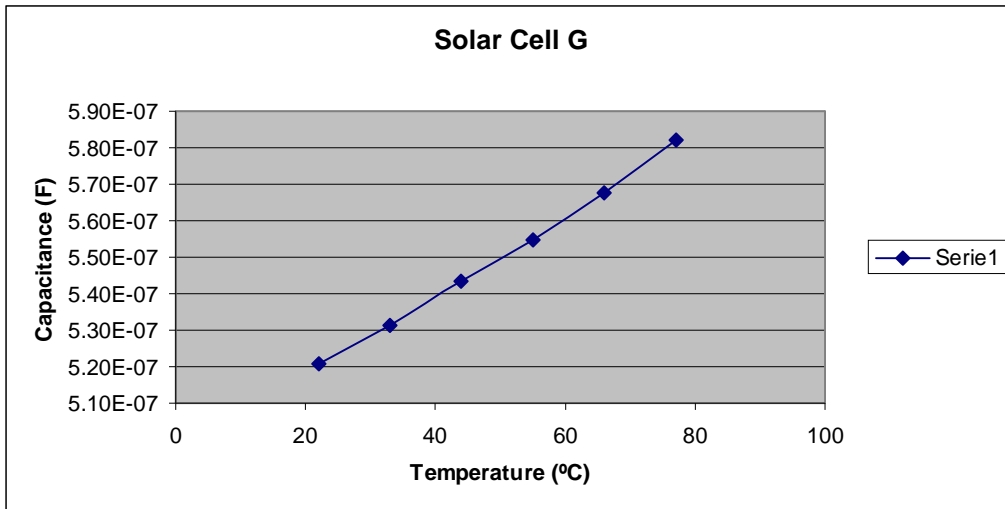


Figure 3.22: Effect of the temperature in solar cell C's capacitance.

Comparison between all the samples:

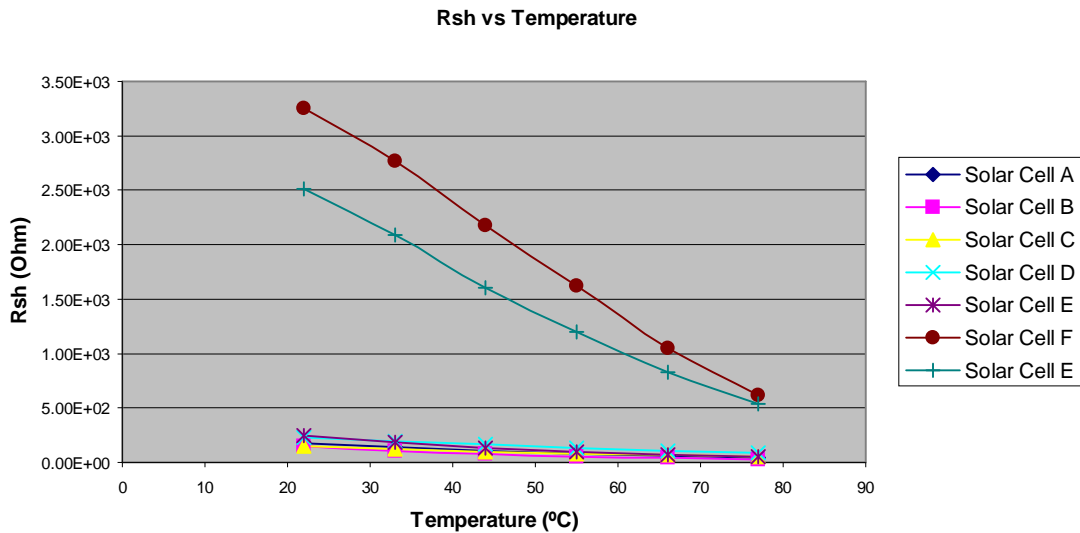


Figure 3.23: Effect of the temperature in  $R_{SH}$  of all the samples.

In the figure 3.23 we can see that the effect of the temperature is higher for the non-concentrated solar cells. The lost of shunt resistance is a lost of efficiency too.

In the parameter tables of solar cells C and G can see the differences between  $R_S$  values. This is the most important electrical parameter, which has influence in the fill factor (therefore in the efficiency too):

$$FF = FF_0 \left( 1 - \frac{R_S \cdot I_{SC}}{V_{OC}} \right) \quad (3.16)$$

Solar cell C(concentrated cell) has a  $R_S$  of the order of  $10^{-3}$  Ohms, on the other hand solar cell G(non concentrated) has a  $R_S$  of the order of  $10^{-2}$ .

We don't have the value of the curve when it cuts the X axis and, as we said before, this is the value of  $R_S$ .



**Rs vs Temperature for all the samples in AC**

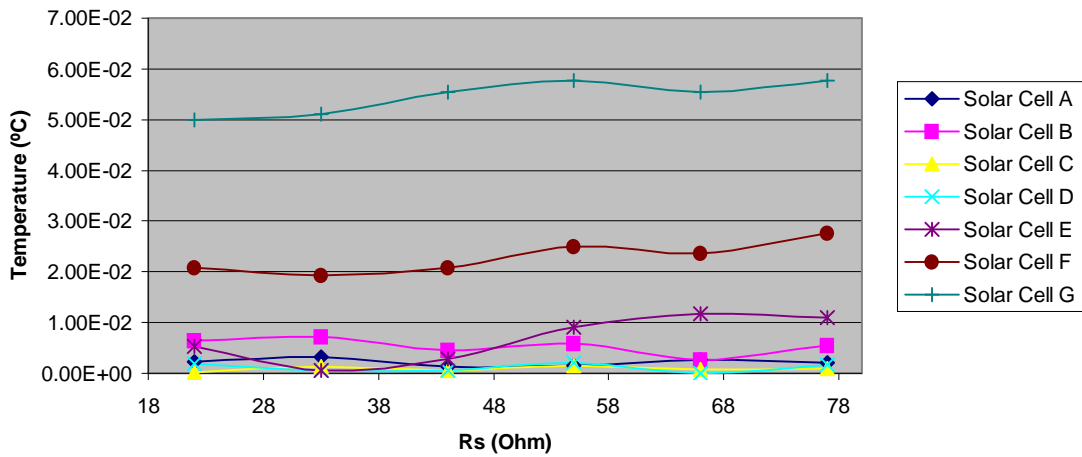


Figure 3.24. Effect of temperature in  $R_s$  in all the samples

As can see in the figure 3.25 the differences in the capacitance between non-concentrated and concentrated ones are big too.

**Capacitance vs Temperature**

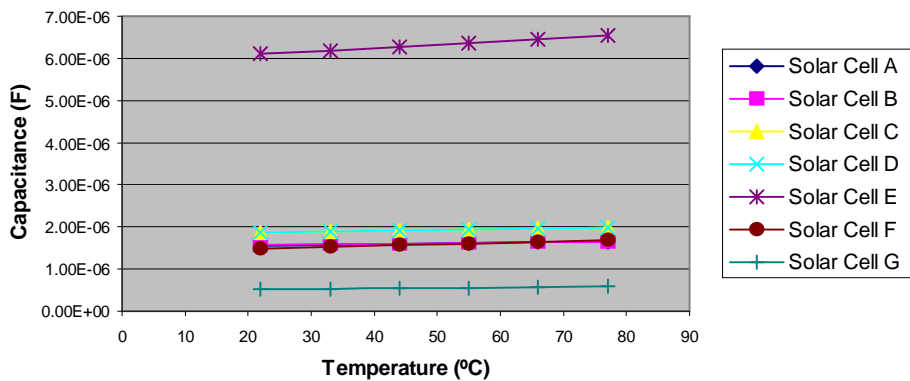


Figure 3.25 : Effect of the temperature in capacitance of all the samples.

The bigger samples E (concentrated) and F (non-concentrated), both of them with the same size, have a big capacitance difference as we can see in the figure 3.25, being the E sample's capacitance much more bigger than F's.

Solar cell G, the non-concentrated and small one, has the lowest capacitance. The increased capacitance has considerable effect on the design of the switching regulators used to regulate the voltage of the solar panels.

For all the samples it was found that the cell capacitance increases with temperature when the cell resistance ( $R_{SH}$ ) decreases.[8]

To calculate  $E_a$ , the equation 3.17 has used:

$$G(f) = G_0 \exp\left(\frac{-Ea}{kT}\right) \quad (3.17)$$

taking  $G(f)$  from the curve between  $G_{SH}=1/R_{SH}$  and  $1/T$  for each cell.

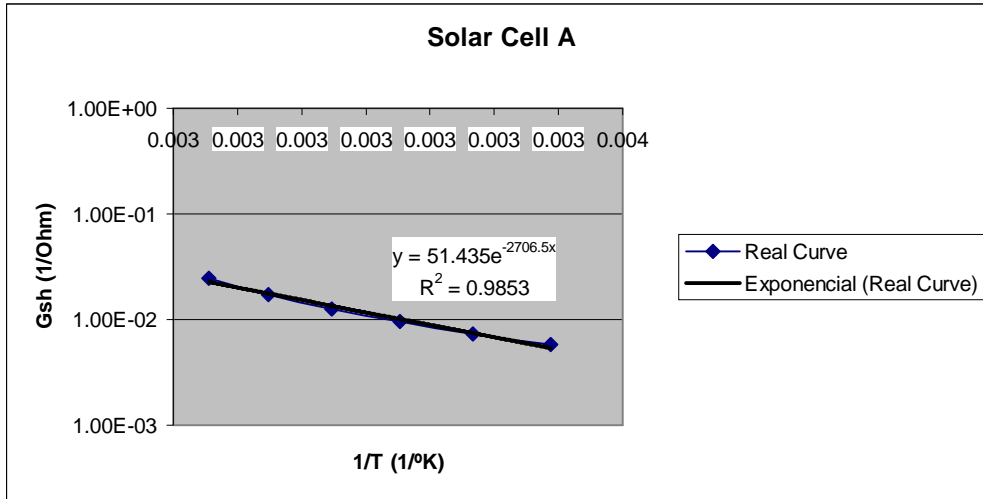


Figure 3.26. Temperature influence in shunt conductivity

	Ea(eV)
Solar Cell A	0.23354563
Solar Cell B	0.25901863
Solar Cell C	0.16019858
Solar Cell D	0.15881793
Solar Cell E	0.25446248
Solar Cell F	0.26312606
Solar Cell G	0.24682576

Figure 3.27: Activation energy ( $E_a$ ) of each sample.

The activation energy can be described as the height of the potential barrier (sometimes called the energy barrier) separating two minima of potential energy. In the solar cells, activation energy, characterizes the activation of the conductivity via the solar cell structure (bulk and surface).

## 4. Conclusions:

The most important thing of a solar cell is its efficiency, or saying it in other words, how solar cell takes the energy coming from the sun and becomes it in electrical energy losing the less of that taking power. To analyze the electrical properties, like  $R_S$ ,  $R_{SH}$  and  $C$ , is a good way to understand how those losses appear.

Two ways to analyze has been used. The first one using dark  $I$ - $V$  technique, and the second one using AC measurement technique, introducing a small signal in dark conditions.

The influence of the temperature has been shown. All the cells have been measured at different temperatures, from 22°C to 77°C, inside an oven with dark  $I$ - $V$  and AC techniques.

The final conclusions are:

1. We have used two diode model for better description of the solar cells behaviour using dark  $I$ - $V$  measurements.
2. For  $R_{SH}$  calculation we have proposed to use AC measurement technique, which has been found to give more appropriate results comparing of DC and AC techniques.
3. The influence of temperature has been shown. As temperature increases the  $R_{SH}$  decreases and  $R_S$  increases. Both resistances influence at the end the efficiency of the solar cells.
4. The  $R_S$  is a current dependent dynamic parameter. The results are highly influenced by the used method and also by the electric (current) conditions of measurements.

The future lines are:

1. To measure I-V curve down toward lower current and voltage results in higher accuracy in the low current zone of dark  $I$ - $V$  measurements. The value of  $R_{SH}$  is going to be more precise. But on the other hand such measurement is demanding more precise (more expensive) apparatus.
2. For high currents in concentrated solar cells it will be necessary to have a programmable power supply with higher current output than 6 amperes which was used. It is necessary when calculating the value of  $R_S$  using data of I-V curve.

## 5. References:

- [1] Luque, Antonio; Hegedus, Steven. Handbook of Photovoltaic Science and Engineering © 2003 John Wiley & Sons
- [2] E. Lorenzo, G. Araujo, A. Cuevas, M. Egido, J. Miñano and R. Zilles. Solar electricity, engineering of photovoltaic systems © 1994
- [3] Stefan C.W. Krauter. Solar Electric Power Generation – Photovoltaic Energy Systems - Modeling of Optical and Thermal Performance, Electrical Yield, Energy Balance, Effect on Reduction of Greenhouse Gas Emissions © 2006 Springer-Verlag Berlin Heidelberg
- [4] Ewa Radziemska Dark I-U-T measurements of single crystalline silicon solar cells. 2004. Energy conversion and Management 46, 1485-1494
- [5] A. Kaminski, J. J. Marchand, A. Laugier. Non ideal dark I-V curves behavior of silicon solar cells. 1998 . Solar Energy Materials and Solar Cells 51, 221-231
- [6] Viktor Schlosser and Ahmed Ghitas. Measurement of silicon solar cells ac parameters. 2006. ARSEC – Bahrain, to be published
- [7] M. Pellegrino, G. Nardelli, A. Sarno. An indoor technique for assessing the degradation of PV modules. 1997. Barcelona – 14<sup>th</sup> European Photovoltaic Conference
- [8] M.S. Suresh. Measurement of solar cell parameters using impedance spectroscopy. 1995. Solar Energy Materials and Solar Cells 43, 21-28
- [9] D. L. King, B. R. Hansen, J. A. Kratochvil and M. A. Quintana. Dark current-voltage measurements of photovoltaic modules as a diagnostic or manufacturing tool. 1997. 26<sup>th</sup> IEEE Photovoltaic Specialist Conference, Anaheim, California
- [10] John H. Scofield. Admittance measurements on Cu(In, Ga)Se<sub>2</sub> Polycrystalline thin film solar cells. 1995. 24<sup>th</sup> IEEE Photovoltaic Specialist Conference, pp. 291-294.
- [11] D. Chenvidya, K. Kirtikara, C. Jivacate. A new characterization method for solar cell dynamic impedance. 2002. Solar Energy Materials & Solar Cells 80 (2003) 459-464
- [12] John H. Scofield. Effects of resistance and inductance on solar cell admittance measurements. Solar Energy Materials and Solar Cells 37(1995) 217-233
- [13] M. Wolf, G.T. Noel, and Richard J. Stirn. Investigation of the double exponential in the current-voltage characteristics of silicon solar cells. IEEE Transactions on electron devices, vol. ED-24, 1997
- [14] Naoki Koide, Ashrafal Islam, Yasuo Chiba, Liyuan Han. Improvement of efficiency of dye-sensitized solar cells based on analysis of equivalent circuit. Journal of Photochemistry and Photobiology A: Chemistry 182, 296-305

## 6. Annex:

```
/*C language program to measure I-V-T curves in dark conditions:*/

//libraries

#include <dos.h>
#include <conio.h>
#include <stdio.h>
#include <stdlib.h>
#include <math.h>
#include <string.h>
#include <gpib.h>

void main(void)
{
    FILE *fp;
    char letter;
    int i=0,j,n,pm,o,pm3,x=0,y=0,z=0;
    float pm_f,k,k1,over_curr_prot, voltage=0, voltage_a, v_apply, voltage_R, R, current, interval_v, v_fix,
a;
    char send_v[20], f, name[10], tmp[10], nap[10];

//initialize
    clrscr();//clear screen
    hp_ifc();//interface clear
    hp_ren1();//remote control enable
    hp_cmd(38);//address of keithleys 619 instrument in listener mode to configurate it
    hp_cmd(97);//channel a, 97 is 'a' in ascii
    //SDC://selected device clear
    //hp_outmes("X");
    //hp_cmd(38);
    //hp_cmd(97);
    hp_outmes("C0");//disable zero check
    hp_outmes("Z0");//disable zero correct
    hp_outmes("F0");//voltage measure
    hp_outmes("R0");//autorange
    hp_outmes("T1");//one shoot talk
    hp_outmes("X");//execute instructions
    delay(2);
    hp_cmd(38);//{ address of keithleys 619 instrument in listener mode to configurate it}
    hp_cmd(98);//{ channel b, 98 is 'b' in ascii}
    hp_outmes("C0");//disable zero check
    hp_outmes("Z0");//disable zero correct
    hp_outmes("F0");//voltage measure
    hp_outmes("R0");//autoRange {since 0'2 A}
    hp_outmes("T1");//one shoot talk
    hp_outmes("X");//{execute instructions}
    delay(2);
    hp_cmd(38);
    UNL;//unlisten
    hp_outmes("X");
    hp_cmd(44);//address of programmable power supply in listener mode to configurate it
    //SDC://selected device clear
    //hp_cmd(44);
    hp_outmes("OCP 1");//set the overcurrent protection
    hp_outmes("ISET 4.5");//sets the maximun current
    delay(2);
```

```

printf("press f to start fixing the voltage or another key to escape\n");
scanf("%c", &f);
if (f=='f')
{
    printf("Write the máximun voltage, it cant be more than 0.8 volt\n");
    scanf("%f", &v_fix);
    if (v_fix>=0.8) v_fix=0.8;
    printf("Write the applied voltage\n");
    scanf("%f", &v_apply);
    printf("Write series resistance value\n");
    scanf("%f",&R);
    printf("Write the amount of measurements\n");
    scanf("%d", &pm);
    j=7;
    while(j>6)
    {
        printf("Write the name of the saving archive - less than 6 letters\n");
        scanf("%s", &name);
        j=strlen(name);
    }
    strcat(name, ".txt");
    fp=fopen(name, "a");
    fprintf(fp,"Name: %s;\nMaximun voltage: %f;\nAmount of
measurements:%d;\n\n", name, v_fix, pm);
    pm_f=pm/3;
    pm3=pm_f;
    while(i<pm)
    {
        /*creating voltage interval*/
        if (voltage_a<0.2)
        {
            k=(x*0.2/pm3);
            x++;
        }
        else
            if ((voltage_a==0.2)|(0.2<voltage_a & voltage_a<0.5))
            {
                k=((y*0.5/pm3)+0.2);
                k1=k;
                y++;
            }
            else
                if ((voltage_a==0.5)|(0.5<voltage_a &
voltage_a<v_fix))
                {
                    k=((z*v_apply/pm3)+k1);
                    z++;
                }
            //printf("%f\n",k);/*save sending voltage into the file*/
            sprintf(tmp,"VSET %f", k);/*put in tmp the message "VSET k(value)"
            //printf("%s\n",tmp);
            hp_cmd(44);
            hp_outmes(tmp);/*send the voltage value to the power supply
            delay(2);
            hp_cmd(44);
            hp_outmes("VSET?");/*ask the value of the applied voltage
            hp_cmd(76);
            sprintf(nap,"%s", hp_inpmes());/*check the value of the applied
voltage
            voltage_a=atof(nap);

```

```

printf("applied voltage %f\n",voltage_a);
hp_cmd(44);
UNL;//unlisten power supply device
delay(2);
hp_cmd(38);
hp_cmd(97);
for (n=0;n<3;n++)
{
    hp_cmd(70);//keithleys address
    hp_cmd(97);//channel a
    sprintf(nap,"%s", hp_inpmes());//read the voltage in the solar
cell
}
for (o=0;o<5;o++)
{
    nap[o]='0';//putting zeros in the first 5 array cells {command
letters}
}
voltage=atof(nap);//convert into float
if (voltage>0.8) break;// protection to safe the solar cell of
overcurrents

printf("voltage %f\n",voltage);
delay(2);
if (current<0.5)//if current is lower than 0'5A it's measured with
keithleys 619
{
    /*if (current>0.2)
    {
        hp_cmd(38);//{ address of keithleys 619 instrument
in listener mode to configurate it}

        hp_cmd(98);//{ channel b, 98 is 'b' in ascii}
        hp_outmes("R9");//configuration in 2 Amps
máximun mode

        hp_outmes("X");//execute
    }*/
    for (n=0;n<3;n++)
    {
        hp_cmd(70);//keithleys address
        hp_cmd(98);//channel b
        sprintf(nap,"%s", hp_inpmes());//get the voltage in
the series resistance
    }
    //printf("%s",nap);
    for (o=0;o<5;o++)
    {
        nap[o]='0';
    }
    voltage_R=atof(nap);//convert into float
    current=voltage_R/R;//get the current with the Ohm law
    printf("current %f\n",current);
    delay(2);
}
else//if current is higher than 0'5 it's measured with the power supply
{
    hp_cmd(38);//deactivate current measuring with keithleys
    hp_cmd(98);
    UNT;
    UNL;
    hp_outmes("X");
    hp_cmd(44);//activate current measuring with power supply

```

```

        hp_outmes("IOUT?");//ask the power supply current
        hp_cmd(76);
        sprintf(nap,"%s", hp_inpmes());//get current from power
supply
        current=atof(nap);
        printf("current %f\n",current);
        delay(2);
        hp_cmd(44);
        UNT;// no sé si está bien. mirarlo
        UNL;// power supply in unlisten mode
    }
    fprintf(fp,"%f    %f    %f\n",voltage_a,voltage,current); //write the
values in the file
        i++;
        hp_cmd(38);
        UNT;
        UNL;
        hp_outmes("X");
        delay(2);
    }
    fprintf(fp,"\n\n\n");
    fclose(fp);//close file
}
hp_cmd(38);
SDC;/* Selected device clear */
GTL;/* Go To Local */
UNL;/* Unlisten */
hp_cmd(44);
SDC;
GTL;
UNL;
hp_ren0();/* Remote Disable */

```